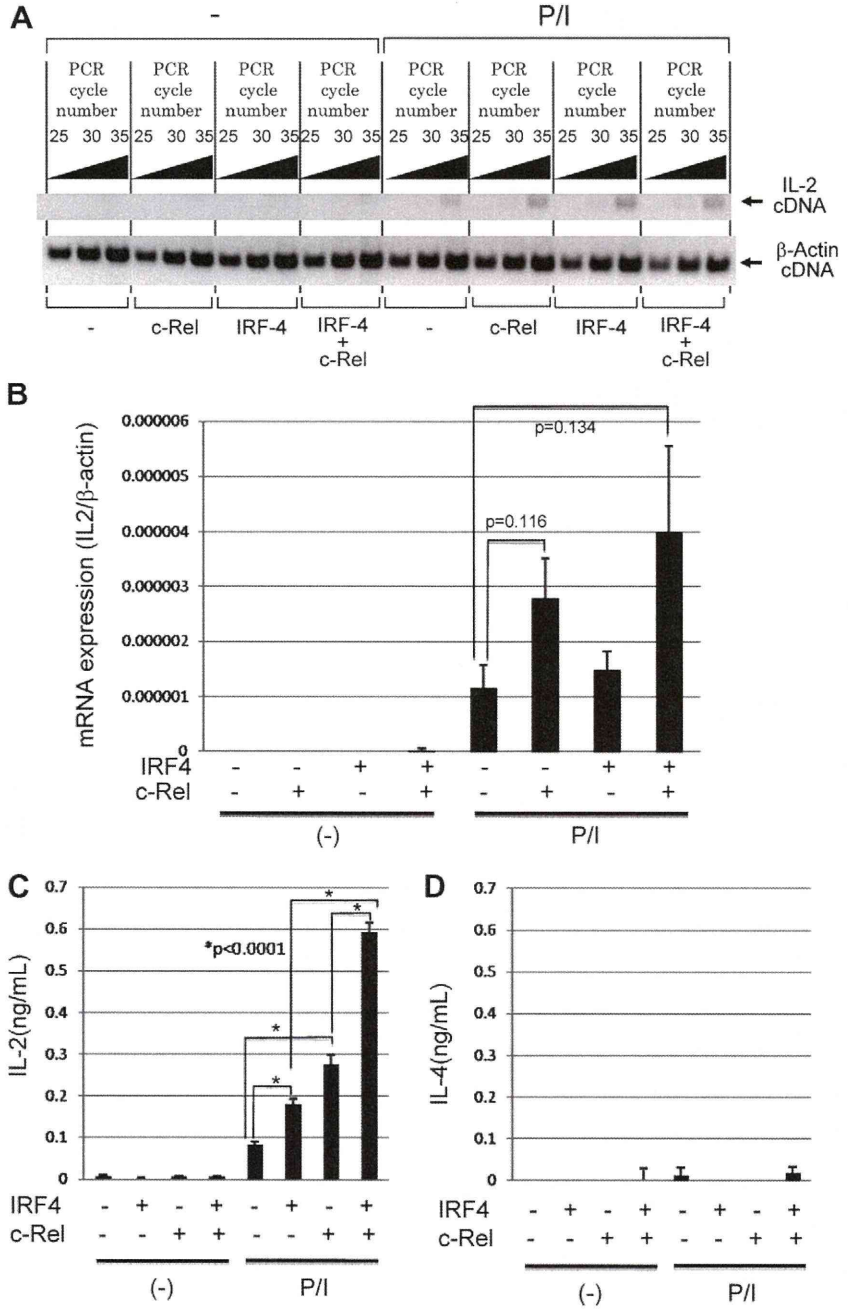


**Fig. 4.** IRF-4 and c-Rel activate the IL-2 promoter to produce IL-2. HUT102 cells ($4 \times 10^5$) were transfected with IRF-4 and c-Rel expression plasmids (2 μg each) by electroporation. Two days after transfection, the cells were incubated for 8 h in the presence or absence of 250 ng/ml PMA and 1 μM Ionomycin (P/I), and the total RNA was extracted. The amounts of IL-2 and β-actin cDNAs were estimated by applying different numbers of PCR cycles (A), and measured by real-time PCR using the specific primers (B). The EL-4 cells ($2 \times 10^5$) were transfected with IRF-4 and c-Rel expression plasmids (500 ng each) by electroporation. Two days after transfection, the cells were incubated for 8 h in the presence or absence of P/I, and the amounts of IL-2 (C), and IL-4 (D) in the supernatant were measured by sandwich ELISA. The data shown are representative of three independent experiments done in triplicate.

the binding was enhanced by the P/I treatment, as compared to the control lanes. The direct binding of IRF-4 and c-Rel each other, their binding to the IL-4 promoter, and the result that the increment of promoter activity by the both IRF-4 and c-Rel transfection (3.47-fold) was larger than the addition of each transfection (0.88-+1.11- = 1.99-fold), suggested that IRF-4 and c-Rel cooperatively activated the IL-4 promoter. However, we could not deny the possibility of that IRF-4 and c-Rel worked independently on the IL-4 promoter activation. The P/I treatment is often used to activate T-cells, as well as the treatments with non-specific mitogens, specific T-cell receptor (TCR) antigens, and the TCR antibodies. The optimal concentration and duration of the reagents were determined by measuring the amounts of mRNA with real-time PCR using specific primer sets for IL-2, and IL-4, as shown in Supplemental Fig. S4. When the EL-4 mouse T-cells were treated with these reagents, Ionomycin only or PMA only was not enough to fully activate IL-2 and IL-4 promoters (Supplemental Fig. 4SA and SD). PMA activated the IL-2 and IL-4 promoters dose-dependently in the presence of 1 μM Ionomycin, and the mRNA expressions reached peak at 8 h (Supplemental Fig. 4SB and SE). The plate-

bound 0.5 μg/ml anti-CD3, and 4 μg/ml anti-CD28 also activated the IL-2 and IL-4 promoters (Supplemental Fig. 4SC and SF). We used 250 ng/ml PMA, and 1 μM Ionomycin, and plate-bound 0.5 μg/ml anti-CD3, and 4 μg/ml anti-CD28 for 4–8 h to activate T-cells otherwise indicated. The treatments with the same amounts of P/I were also employed to stimulate effectively $CD4^+$ T-cells, and HUT102 cells.

### 3.4. IRF-4 and c-Rel activate the IL-2 promoter to produce IL-2

IRF-4 is reported to stimulate IL-2 production as well as IL-4 [14]. To examine the effects of IRF-4 and c-Rel on the IL2-promoter, we introduced the plasmids encoding IRF-4 and c-Rel into HUT102 cells. We estimated the amount of IL-2 cDNA by applying different numbers of PCR cycles, after converting the mRNA to cDNA by reverse transcriptase, and evaluating the amount of β-actin cDNA as the total amount of mRNA. As shown in Fig. 4A, substantial amounts of IL-2 cDNA were detected in the presence of P/I, as compared to those in the absence of P/I, and the amount of IL-2 cDNA was increased by exogenously expressing c-Rel or IRF-4. To assess the data quantitatively, we employed the real-time PCR using IL-2 specific primers, and measured the mRNA expression of IL-2 relative to β-Actin (Fig. 4B). In the presence of P/I, the exogenous IRF-4 and c-Rel appeared to increase the expression of IL-2 mRNA, but the enhancing effects were not significant ($p = 0.116$ and 0.134). We think that the cooperation of IRF-4 with c-Rel was not observed, because HUT102 cells express a large amount of IRF-4, and thus the increases of IL-2 cDNA by IRF-4 or c-Rel were relatively small. Indeed, in EL-4 cells, a cooperative effect of IRF-4 with c-Rel on IL-2 production was observed, by measuring the amounts of IL-2 produced from the cells transfected with the plasmids encoding IRF-4 and c-Rel, using an ELISA (Fig. 4C). However, any detectable amounts of IL-4 were not produced by any combinations of the reagents (Fig. 4D). The roles of IRF-4 and c-Rel in

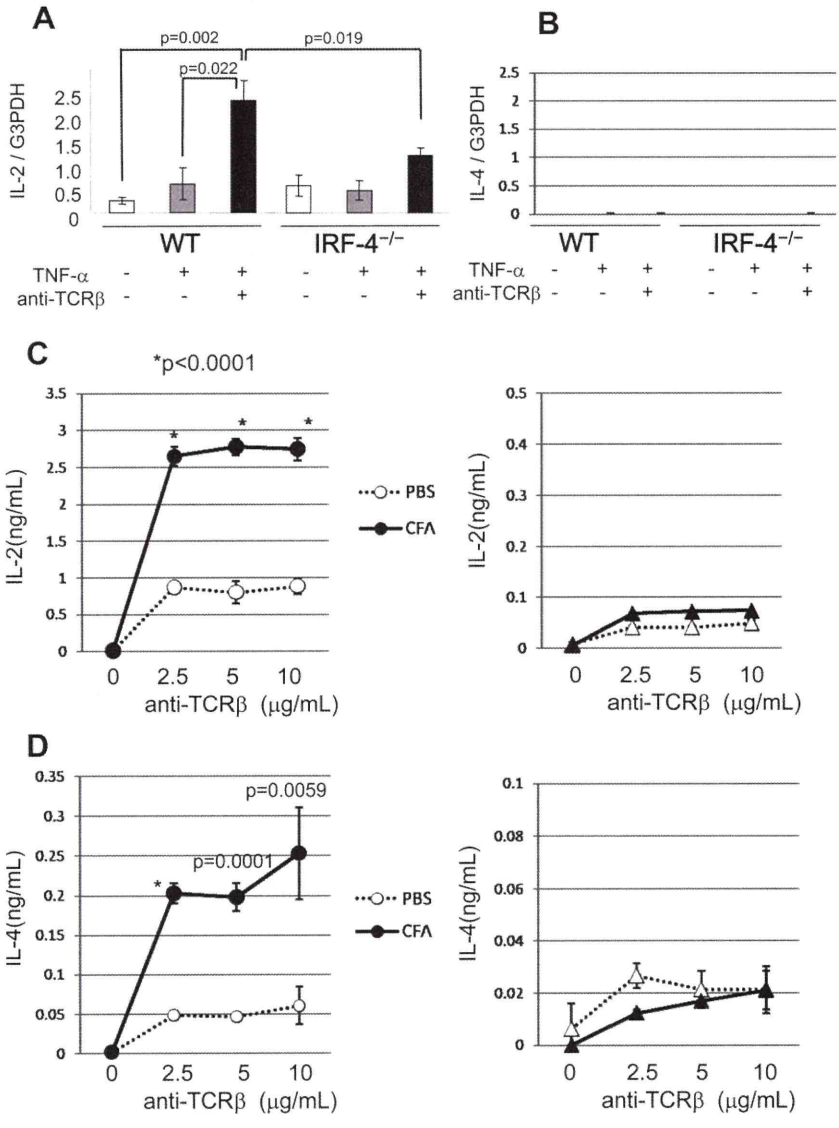


**Fig. 5.** IRF-4 is indispensable to produce IL-2 and IL-4 production *in vivo*. (A and B) TNF-α-mediated priming of naive T-cells requires IRF-4. $CD4^+$ T-cells were purified from the spleens of C57BL/6 mice (WT) or IRF-$4^{-/-}$ mice, and were activated with 5 ng/ml of TNF-α or with TNF-α plus anti-CD3 antibody (10 μg/ml) for 6 h. The relative amounts of IL-2 (A) and IL-4 (B) mRNA normalized to the quantity of G3PDH mRNA were determined by real-time PCR, using the reverse-transcribed cDNAs. The data shown are representative of three independent experiments done in triplicate. (C and D) Adjuvant-mediated priming of naive T-cells also requires IRF-4. C57BL/6 mice (WT) and IRF-$4^{-/-}$ mice were injected intraperitoneally with complete Freund's adjuvant (CFA) or saline (PBS), followed by a second injection of incomplete Freund's (IFA) or PBS, respectively. Six days later, splenic T-cells were activated with various amounts of plate-bound anti-TCRβ antibody, and the levels of IL-2 (C), and IL-4 (D) were determined by an ELISA. Data shown are representative of three independent experiments.

IL-2 and IL-4 promoter activations are different in cell types and specific conditions. For example, c-Rel is indispensable for the optimal IL-2 production in naïve T-cells, but is not required in for the IL-2 production in blast T-cells [19]. IRF-4 is also reported to differentially regulates the production of Th2 cytokines including IL-4 in naïve vs. effector/memory $CD4^+$ T-cells [20]. The specific roles of the c-Rel and IRF-4 interaction in the activation of the IL-2 and IL-4 promoters should be elucidated in specific cells and proper conditions.

### 3.5. Optimal IL-2 and IL-4 productions require IRF-4 in vivo

Next, we examined the effects of IRF-4 on IL-2 and IL-4 productions *in vivo* using IRF-$4^{-/-}$ mice, because the IRF-4 and c-Rel interaction reminded us of the similar T-cell phenotypes between IRF-$4^{-/-}$ mice and c-$Rel^{-/-}$ mice (both mice exhibited defects in T-cell proliferation and IL-2 production in response to anti-CD3 stimulation). In addition, Banerjee et al. reported that cytokine-mediated priming of naïve T-cells was c-Rel-dependent [19]. Therefore, we measured the IL-2 and IL-4 expressions in splenic $CD4^+$ T-cells from normal and IRF-$4^{-/-}$ mice, by anti-CD3 stimulation with and without TNF-α pretreatment. The amount of IL-2 mRNA in IRF-4-deficient cells (IRF-$4^{-/-}$) was significantly lower than that in normal cells, as evaluated by quantitative real-time PCR (WT) (Fig. 5A). These results indicated that not only c-Rel but also IRF-4 is required for the optimal production of IL-2 in TNF-α-primed T-cells. On the other hand, we could not detect any IL-4 mRNA by anti-CD3 stimulation even in TNF-α-primed T-cells from WT or IRF-$4^{-/-}$ mice (Fig. 5B).

We further examined the effects of complete Freund's adjuvant (CFA)-mediated priming on the IL-2 production in splenic $CD4^+$ T-cells. Naive T-cells from CFA-primed normal (WT), but not IRF-$4^{-/-}$, mice produced high levels of IL-2 in response to anti-CD3 stimulation (termed superinduction), dependent on the amount of TCRβ antibody (Fig. 5C). The priming effect of CFA was completely absent in the IRF-4-deficient T-cells. To elucidate the mechanism of high IL-2 production, we examined the priming effects on the IL-2 promoter activity by measuring IL-2 mRNA with real-time PCR (Fig. 6A). The IL-2 mRNA amounts enhanced by TCR stimulation with the anti-CD3 and anti-CD28 antibodies were CFA-dependent

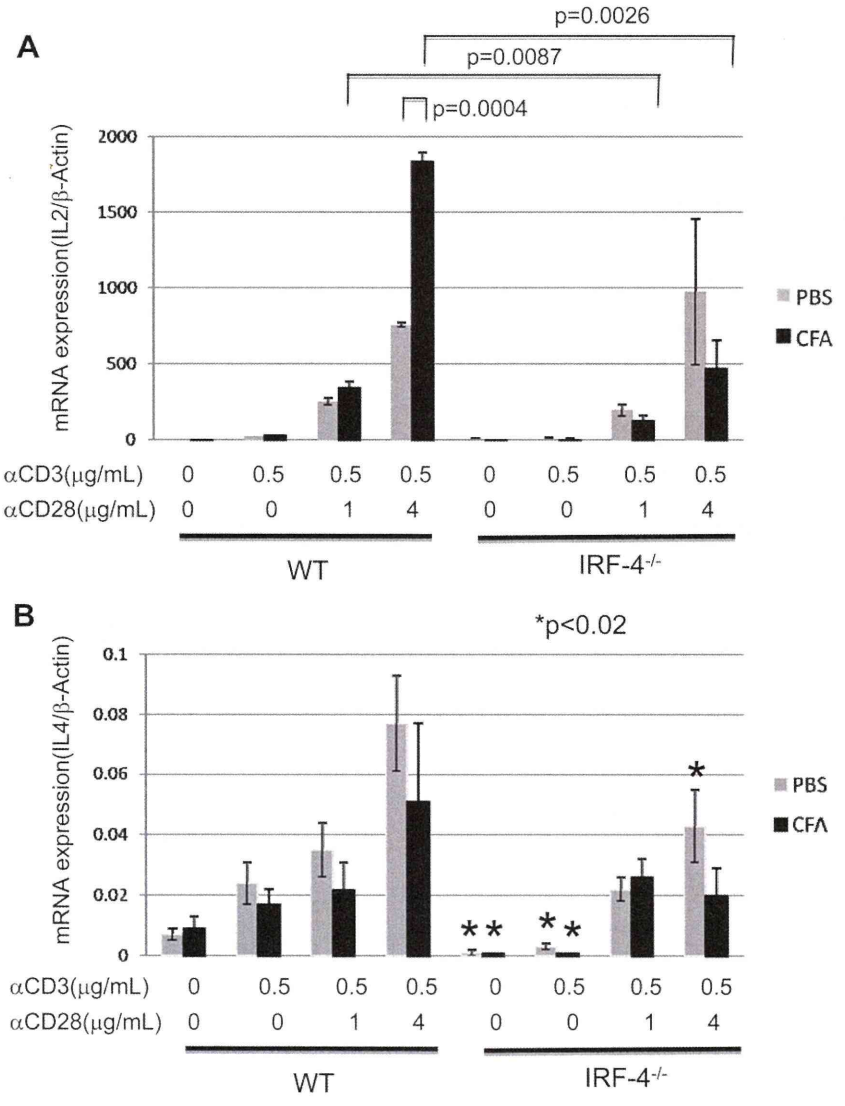


**Fig. 6.** Effects of IRF-4 on the IL-2 and IL-4 promoters *in vivo*. C57BL/6 mice (WT) and IRF-$4^{-/-}$ mice were injected intraperitoneally with complete Freund's adjuvant (CFA) or saline (PBS), followed by a second injection of incomplete Freund's (IFA) or PBS, respectively. Six days later, splenic T-cells were activated with various amounts of plate-bound anti-CD3, and anti-CD28 antibodies, and the relative amounts of IL-2 mRNA (C), and IL-4 mRNA (D) normalized to the quantity of β-Actin mRNA were determined by real-time PCR. Data shown are representative of three independent experiments.

in the WT mice-derived $CD4^+$ T-cells. The CFA-dependent superinduction was disappeared in IRF-$4^{-/-}$ mice, as reported in c-$Rel^{-/-}$ mice. These indicated that IRF-4 as well as c-Rel is indispensable to fully activate IL-2 promoter *in vivo*.

As for IL-4 regulation, the IL-4 production stimulated with TCRβ antibody was also dependent on the CFA priming in WT, although the amounts of IL-4 were much smaller than those of IL-2 (Fig. 5C and D). The TCR activation-dependent IL-4 mRNA amounts were significantly lower in the IRF-$4^{-/-}$ mice compared to WT mice, but the CFA-dependence was not observed (Fig. 6B). These suggested that the regulations of IRF-4 may be different in the IL-2 and IL-4 promoters. The discrepancy between the protein and mRNA levels of IL-4 may be caused by the effects of IRF-4 on the stability of IL-4 protein, in addition to the effects on the promoter. Another possibility of the discrepancy between the IL-4 protein and mRNA levels was due to the different sensitivities of the detection systems employed here. The differences in mRNA expression measured at 4 h after TCR stimulation may be not enough to assess the IL-4 promoter activities, considering that the IL-4 protein levels measured by ELISA reflect the continuous effects during 16 h, and that the differences of IL-4 amounts were much smaller than those of IL-2.

## 4. Discussion

In the present study, we isolated a protein complex associated with IRF-4 in HTLV-1-infected T-cells using the TAP method, and showed that an NF-κB family member, c-Rel, physically associates with IRF-4 and enhances the IRF-4-dependent IL-4 and IL-2 promoter activation in some T-cells. In addition, we mapped their binding sites to the C-terminal IRF association domain of IRF-4, and the N-terminal Rel-homology domain of c-Rel (Fig. 2). Considering that these domains are used for interactions with other IRF members and NF-kB members, respectively, their interactions may affect the various functions of important transcription factors involved in cell growth, cell death, immunity, and other phenomena [1,21]. Although FKBP52, PU.1, E47, BCL6, STAT6, NFATc2, NFATc1, IBP, and MyD88 have been reported to bind to IRF-4 so far [9,13,21–23], the interaction of IRF-4 with c-Rel and their functional cooperation to enhance the IL-2 and IL-4 promoter activities (Figs. 3 and 4) are noteworthy. IRF-4 was indispensable for the optimal IL-2 and IL-4 productions *in vivo* was evident (Figs. 5 and 6), although the precise mechanism of the cooperation between IRF-4 and c-Rel in the regulation of the cytokine productions should be elucidated. First, the elevated expression of IRF-4 and c-Rel is closely correlated with the exacerbation of ATLL [24] and antiviral therapy resistance in ATLL [15]. The antiviral therapy consists of azidothymidine (AZT) and IFNα, which work at various points to prevent virus infection and proliferation. Considering the fact that the IFNα pathway can cross-talk with the IFNγ pathway [25], one possible mechanism related to the antiviral resistance is that IRF-4 antagonizes the INFγ-mediated IRF1-dependent suppression of the IL-4 promoter [26], by interacting with each other through the IRF association domains, or competing with each other for binding to the same DNA sites (IFN-stimulated response elements (ISREs) are located at the proximal region of IL-4 promoter) (Fig. 3B) or a common adaptor, MyD88 [23]. On the other hand, c-Rel and IRF-4 themselves reportedly activate the IRF-4 promoter [8,27]. The enhancing loop and their cooperation may effectively activate the downstream genes, including the strong T-cell growth factor IL-2 (Fig. 4) and the proto-oncogene c-myc [8]. The determination of the interacting sites between IRF-4 and c-Rel will give precious information to develop specific reagents inhibiting T-cell growth in ATLL patients.

Second, the IRF-4-dependent IL-4 induction in the presence of P/I was reportedly enhanced by the calcineurin-regulated transcription factors NFATc2 (NFAT1) and/or NFATc1 (NFAT2), and may partly explain the crucial roles of IRF-4 in Th2 differentiation [9,12,25]. However, we could not detect any specific binding of endogenous IRF-4 or c-Rel with NFATc1 or NFATc2 in the presence or absence of P/I treatment in HUT102 or EL-4 T-cells, although the exogenously-expressed NFATc1 and NFATc2 showed very weak binding to IRF-4 even in the presence of P/I in 293T cells (data not shown). Considering the redundant and complicated effects of NFAT protein families (NFATc1, NFATc2, and NFAT4 are expressed in T-cells) [28] on the IL-4 promoter activity, and that the substantial interaction of IRF-4 with c-Rel to activate the IL-4 promoter did not require P/I treatment (Figs. 1–3), we think the P/I-dependent enhancement is not simply because of the binding of IRF-4 with the NFATs. IRF-4 was indispensable for the optimal IL-4 production, but the mechanism was not explained only by the effects on the IL-4 promoter activation (Figs. 4–6).

In contrast, our data suggested that IRF-4 worked mainly on the IL-2 promoter activation, and the activation was may be in cooperation with c-Rel. The IL-2 promoter activation by IRF-4 required P/I treatment or TCR stimulation with cytokine priming (Figs. 4–6). These results suggested that qualitative changes of IRF-4 and/or c-Rel, their possible interacting molecules, and the chromatin structure in the IL-2 proximal promoter region by such as phosphorylation, acetylation, and demethylation may be necessary for optimal IL-2 promoter activation [29]. The absence of ISRE site in the IL-2 proximal promoter region, compared to the IL-4 promoter, may be involved in the difference. In addition, c-Rel was recently reported to be required for the development of thymic $Foxp3^+$ CD4 regulatory T-cells (Treg) [30], and Foxp3-dependent IRF-4 induction in Treg is thought to be important for the Treg function to control the Th2 response [31]. Therefore, regulating the interaction between IRF-4 and c-Rel by manipulating the molecules may help to differentiate from pluripotent T-cells into specific lineage to treat various diseases [32].

In conclusion, the elucidation of the physical and functional cooperation between IRF-4 and c-Rel to activate of the IL-4 and IL-2 genes in T-cells is important for future gene therapy for ATLL by abolishing their growth effects, and to present promising targets for adoptive immunotherapy by regulating specific T-cell development.

## Acknowledgements

We thank R. Moriuchi, and H. Udono and T. Mori (Nagasaki University Graduate School of Biomedical Sciences) for the TAP tag expression plasmid, and for LC/MS/MS technical assistance, respectively; S. Yamaoka (Tokyo Medical Dental University School of Medicine) for the human c-Rel expressing plasmid and the 293T cell line; and T. W. Mak (Ontario Cancer Institute, Amgen Institute) for the anti-IRF-4 rabbit polyclonal antibody. This work was supported by Grants-in-Aid from the Ministry of Education, Culture, Sports, Science and Technology of Japan, and by the Global Center of Excellence Program at Nagasaki University.

## Appendix A. Supplementary data

Supplementary data associated with this article can be found, in the online version, at doi:10.1016/j.cyto.2011.08.014.

## References

[1] Savitsky D, Tamura T, Yanai H, Taniguchi T. Regulation of immunity and oncogenesis by the IRF transcription factor family. Cancer Immunol Immunother 2010;59:489–510.
[2] Matsuyama T, Grossman A, Mittrucker HW, et al. Molecular cloning of LSIRF, a lymphoid-specific member of the interferon regulatory factor family that binds

the interferon-stimulated response element (ISRE). Nucleic Acids Res 1995;23:2127–36.
[3] Eisenbeis CF, Singh H, Storb U. Pip, a novel IRF family member, is a lymphoid-specific, PU.1-dependent transcriptional activator. Genes Dev 1995;9:1377–87.
[4] Yamagata T, Nishida J, Tanaka S, et al. A novel interferon regulatory factor family transcription factor, ICSAT/Pip/LSIRF, that negatively regulates the activity of interferon-regulated genes. Mol Cell Biol 1996;16:1283–94.
[5] Mittrucker HW, Matsuyama T, Grossman A, et al. Requirement for the transcription factor LSIRF/IRF4 for mature B and T lymphocyte function. Science 1997;275:540–3.
[6] Brass AL, Zhu AQ, Singh H. Assembly requirements of PU.1-Pip (IRF-4) activator complexes: inhibiting function in vivo using fused dimmers. EMBO J 1999;18:977–91.
[7] Shaffer AL, Emre NC, Romesser PB, Staudt LM. IRF4: Immunity. Malignancy! Therapy? Clin Cancer Res 2009;15:2954–61.
[8] Shaffer AL, Emre NC, Lamy L, et al. IRF4 addiction in multiple myeloma. Nature 2008;454:226–31.
[9] Rengarajan J, Mowen K, McBride K, Smith E, Singh H, Glimcher L. Interferon regulatory factor 4 (IRF4) interacts with NFATc2 to modulate interleukin 4 gene expression. J Exp Med 2002;195:1003–12.
[10] Tominaga N, Ohkusu-Tsukada K, Udono H, Abe R, Matsuyama T, Yui K. Development of Th1 and not Th2 immune responses in mice lacking IFN-regulatory factor-4. Int Immunol 2003;15:1–10.
[11] Suzuki S, Honma K, Matsuyama T, et al. Critical roles of interferon regulatory factor 4 in CD11b high CD8alpha-dendritic cell development. Proc Natl Acad Sci USA 2004;101:8981–6.
[12] Gilmour J, Lavender P. Control of IL-4 expression in T helper 1 and 2 cells. Immunology 2008;124:437–44.
[13] Mamane Y, Sharma S, Petropoulos L, Lin R, Hiscott J. Posttranslational regulation of IRF-4 activity by the immunophilin FKBP52. Immunity 2000;12:129–40.
[14] Hu CM, Jang SY, Fanzo JC, Pernis AB. Modulation of T cell cytokine production by interferon regulatory factor-4. J Biol Chem 2002;277:49238–46.
[15] Ramos JC, Ruiz Jr P, Ratner L, et al. IRF-4 and c-Rel expression in antiviral resistant adult T-cell leukemia/lymphoma. Blood 2007;109:3060–8.
[16] Puig O, Caspary F, Rigaut G, et al. The tandem affinity purification (TAP) method: a general procedure of protein complex purification. Methods 2001;24:218–29.
[17] Brownell E, Mittereder N, Rice NR. A human rel proto-oncogene cDNA containing an Alu fragment as a potential coding exon. Oncogene 1989;4:935–42.
[18] Müller MM, Schreiber E, Schaffner W, Matthias P. Rapid test for in vivo stability and DNA binding of mutated octamer binding proteins with 'mini-extracts' prepared from transfected cells. Nucleic Acids Res 1989;17:6420.
[19] Banerjee D, Liou HC, Sen R. C-Rel-dependent priming of naive T cells by inflammatory cytokines. Immunity 2005;23:445–58.
[20] Honma K, Kimura D, Tominaga N, Miyakoda M, Matsuyama T, Yui K. Interferon regulatory factor 4 differentially regulates the production of Th2 cytokines in naive vs. effector/memory CD4+ T cells. Proc Natl Acad Sci USA 2008;105:15890–5.
[21] Honda K, Taniguchi T. IRFs: master regulators of signalling by Toll-like receptors and cytosolic pattern-recognition receptors. Nat Rev Immunology 2006;6:644–58.
[22] Chen Q, Yang W, Gupta S, et al. IRF-4-binding protein inhibits interleukin-17 and interleukin-21 production by controlling the activity of IRF-4 transcription factor. Immunity 2008;29:899–911.
[23] Negishi H, Ohba Y, Yanai H, et al. Negative regulation of Toll-like-receptor signaling by IRF-4. Proc Natl Acad Sci USA 2005;102:15989–94.
[24] Imaizumi Y, Kohno T, Yamada Y, et al. Possible involvement of interferon regulatory factor 4 (IRF4) in a clinical subtype of adult T-cell leukemia. Jpn J Cancer Res 2001;92:1284–92.
[25] Schroder K, Hertzog PJ, Ravasi T, Hume DA. Interferon-gamma: an overview of signals, mechanisms and functions. J Leukoc Biol 2004;75:163–89.
[26] Li-Weber M, Krammer PH. Regulation of IL4 gene expression by T cells and therapeutic perspectives. Nat Rev Immunol 2003;3:534–43.
[27] Grumont RJ, Gerondakis S. Rel induces interferon regulatory factor 4 (IRF-4) expression in lymphocytes: modulation of interferon-regulated gene expression by rel/nuclear factor kappaB. J Exp Med 2000;191:1281–92.
[28] Macian F. NFAT proteins: key regulators of T-cell development and function. Nat Rev Immunol 2005;5:472–84.
[29] Kim HP, Imbert J, Leonard WJ. Both integrated and differential regulation of components of the IL-2/IL-2 receptor system. Cytokine Growth Factor Rev 2006;17:349–66.
[30] Isomura I, Palmer S, Grumont RJ, et al. c-Rel is required for the development of thymic Foxp3+ CD4 regulatory T cells. J Exp Med 2009;206:3001–14.
[31] Zheng Y, Chaudhry A, Kas A, et al. Regulatory T-cell suppressor program co-opts transcription factor IRF4 to control T(H)2 responses. Nature 2009;458:351–6.
[32] Kim PS, Ahmed R. Features of responding T cells in cancer and chronic infection. Curr Opin Immunol 2010;22:223–30.

Molecular Cell
Article

# Methionine Adenosyltransferase II Serves as a Transcriptional Corepressor of Maf Oncoprotein

Yasutake Katoh,[1,2] Tsuyoshi Ikura,[1,6] Yutaka Hoshikawa,[3] Satoshi Tashiro,[4] Takashi Ito,[5] Mineto Ohta,[1] Yohei Kera,[1] Tetsuo Noda,[3] and Kazuhiko Igarashi[1,2,*]
[1]Department of Biochemistry
[2]Center for Regulatory Epigenome and Diseases
Tohoku University Graduate School of Medicine, Sendai, Miyagi 980-8575, Japan
[3]Genome Center, Japanese Foundation for Cancer Research, Kotoku, Tokyo 135-8550, Japan
[4]Department of Cellular Biology, RIRBM, Hiroshima University, Hiroshima 734-8553, Japan
[5]Department of Biochemistry, Nagasaki University School of Medicine, Nagasaki 852-8523, Japan
[6]Present address: Department of Mutagenesis, Radiation Biology Center, Kyoto University, Kyoto 606-8501, Japan
*Correspondence: igarashi@med.tohoku.ac.jp
DOI 10.1016/j.molcel.2011.02.018

## SUMMARY

**Protein methylation pathways comprise methionine adenosyltransferase (MAT), which produces *S*-adenosylmethionine (SAM) and SAM-dependent substrate-specific methyltransferases. However, the function of MAT in the nucleus is largely unknown. MafK represses or activates expression of heme oxygenase-1 (HO-1) gene, depending on its heterodimer partners. Proteomics analysis of MafK revealed its interaction with MATIIα, a MAT isozyme. MATIIα was localized in nuclei and found to form a dense network with chromatin-related proteins including Swi/Snf and NuRD complexes. MATIIα was recruited to Maf recognition element (MARE) at HO-1 gene. When MATIIα was knocked down in murine hepatoma cell line, expression of HO-1 was derepressed at both basal and induced levels. The catalytic activity of MATIIα, as well as its interacting factors such as MATIIβ, BAF53a, CHD4, and PARP1, was required for HO-1 repression. MATII serves as a transcriptional corepressor of MafK by interacting with chromatin regulators and supplying SAM for methyltransferases.**

## INTRODUCTION

Metabolic flux regulation by compartmentalization of enzymes and substrate channeling is a common theme in many enzymatic pathways. It is becoming clear that some metabolic enzymes related to gene regulation are compartmentalized in nuclei (Hall et al., 2004; Takahashi et al., 2006; Wellen et al., 2009). For example, yeast acetyl-CoA synthetase-2 (ACS2), which catalyzes the synthesis of metabolic intermediate acetyl-CoA, is present in nuclei to provide acetyl-CoA for histone acetylation (Takahashi et al., 2006). Another metabolic intermediate important for gene regulation is obviously *S*-adenosylmethionine (SAM) as a methylation donor (Lu and Mato, 2008). Methylation at cytosine of DNA and at arginine and lysine residues of various proteins including histones are catalyzed by specific methyltransferases using SAM as a methyl donor (Dillon et al., 2005; Goll and Bestor, 2005; Shi, 2007). In contrast to the case of nuclear protein acetylation, how SAM is provided to nuclear methyltransferases is not clear.

Methionine adenosyltransferase (MAT) is a cellular enzyme that catalyzes the formation of SAM from methionine and ATP. Three distinct forms of MAT (MATI, MATII, and MATIII), encoded by two distinct genes (*MAT1A* and *MAT2A*), have been identified in mammals (Sakata et al., 1993, 2005). MATI and MATIII are a tetramer and a dimer, respectively, of $\alpha_1$ catalytic subunit, which is encoded by *MAT1A*. MATIIα, the catalytic subunit of MATII, is encoded by *MAT2A* and forms a dimer, and its activity is inhibited by MATIIβ regulatory subunit encoded by *MAT2B*. While MATI/III is expressed at high levels in adult liver, MATIIα is widely expressed (Kotb et al., 1997; Halim et al., 2001; LeGros et al., 2001). While MATI/III have been reported to be present in nuclei (Reytor et al., 2009), function of MATI/III or MATII in terms of gene regulation is not yet clear.

The small Maf oncoproteins, MafG, MafK, and MafF, possess a basic region-leucine zipper (bZip) domain for dimer formation and DNA binding (Fujiwara et al., 1993; Kataoka et al., 1995; Igarashi et al., 1995). They repress or activate transcription depending on the dimeric partner. For example, MafK-Bach1 heterodimer and MafK-p45 heterodimer (i.e., NF-E2) serve as a repressor and an activator of globin genes, respectively, during erythroid differentiation (Andrews et al., 1993; Igarashi et al., 1994; Oyake et al., 1996; Motohashi et al., 2000; Brand et al., 2004; Tahara et al., 2004a, 2004b). In diverse types of cells, MafK-Bach1 represses expression of subset of oxidative stress-inducible genes such as heme oxygenase-1 (HO-1) and ferritins (Sun et al., 2002, 2004; Igarashi and Sun, 2006; Hintze et al., 2007), whereas heterodimer of MafK and NF-E2-related factor 2 (Nrf2) activates their expression (Itoh et al., 1997; Zhang et al., 2006). In B cells, MafK-Bach2 heterodimer represses the transcription of Blimp-1 gene, a master regulator of plasma cell differentiation (Muto et al., 1998, 2004; Ochiai et al., 2006, 2008). Small Maf heterodimers bind to their target genes by recognizing specific DNA sequences termed Maf recognition

elements (MAREs) (Kataoka et al., 1995). However, molecular mechanisms by which these heterodimers repress or activate target genes are still unclear.

We purified MafK complex from mouse plasmacytoma cell line X63/0 with an aim to understand its protein network. MATIIα was identified in the purified MafK complex by mass spectrometry analysis. We further purified MATIIα, revealing its interaction with components of Polycomb group (PcG), NuRD, Swi/Snf, and PARP complexes. We demonstrated that both MATIIα and MATIIβ were recruited to MARE of the HO-1 gene. The enzymatic activity of MATIIα, as well as its interacting proteins including MATIIβ and CHD4, was required for the HO-1 repression. Purified MATIIα associating with MATIIβ and other factors catalyzed SAM synthesis and histone methylation in vitro. Therefore, MATIIα and -β within this higher-order oligomer were named a SAM-integrating transcription regulation (SAMIT) module. We suggest that MATII serves as a transcription corepressor of MafK by providing SAM locally and interacting with chromatin-related factors.

## RESULTS

### Proteomic Analysis of MafK Network

To understand the protein network involving MafK, we purified MafK complexes from mouse plasmacytoma (X63/0) cells stably expressing FLAG-HA-His epitope-tagged MafK (eMafK). The expression level of eMafK in X63/0 cells was similar to that of endogenous MafK (data not shown). eMafK was purified from nuclear extracts by two-step immunoaffinity chromatography (see the Experimental Procedures; Figure 1A, lane 2). As a control, we performed a mock purification from nuclear extracts prepared from nontransduced X63/0 cells (Figure 1A, lane 1). As shown in Figure 1A, the purified eMafK fraction contained several other proteins at varying stoichiometric ratios. We employed mass spectrometry to identify these proteins. The presence of Bach1 and endogenous MafK verified the purification procedure because MafK forms a heterodimer with Bach1 or a homodimer (Table S1, Figures 1A and 1B). There were at least 11 bands that appeared specific because they were present in several independently purified samples but were absent in mock purification. A list of identified proteins is provided as Table S1, available online. MafK-interacting proteins included facilitates chromatin transcription (Supt16h/Fact140), poly(adenosine diphosphate-ribose) polymerase-1 (PARP1), Ku80, Ku70, and MATIIα. The presence of identified proteins including MATIIα in the MafK complex was confirmed by immunoblot analysis (Figure 1B). Using the Bach1 complex purified and characterized from murine erythroleukemia (MEL) cells (Dohi et al., 2008), we found that MATIIα was present in this complex by mass spectrometry and immunoblot analyses (Figure 1C and data not shown). To verify the specificity of MafK-MATIIα interaction, we carried out an immunoprecipitation analysis of endogenous proteins in mouse hepatoma (Hepa1) cells (Figure 1D) and found that MATIIα was coimmunoprecipitated with MafK (Figure 1D, middle panel). The expression of MATIIα was detected in X63/0 plasmacytoma cells, MEL, Hepa1 cells, and murine embryonic fibroblasts (MEFs), showing a wide distribution (Figure S1). These results raised the possibility that MATIIα interacted directly or indirectly with MafK and/or Bach1 in various tissues or cells.

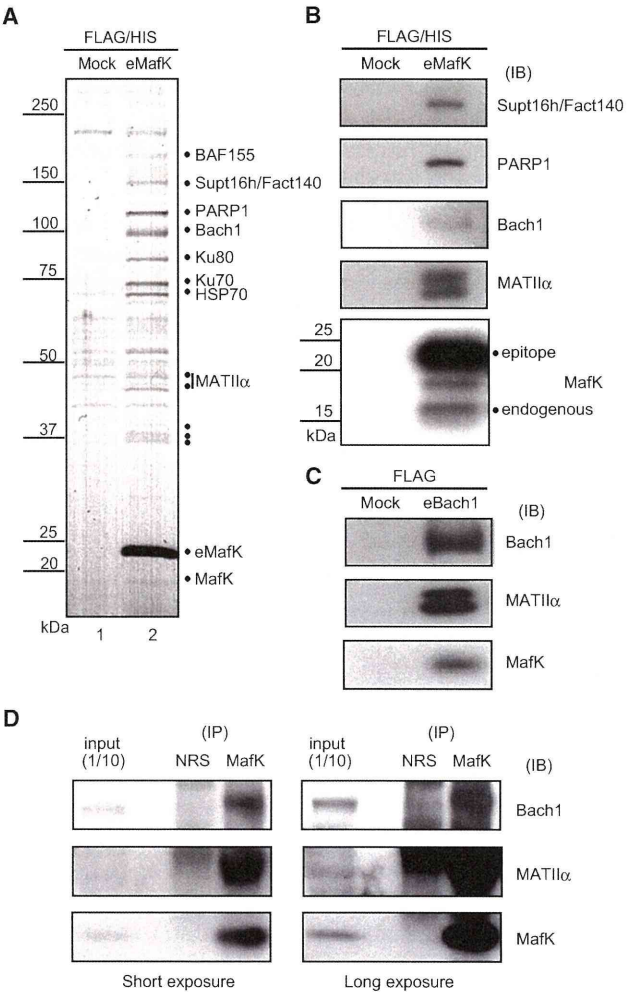


**Figure 1. Purification of MafK Complex**

(A) MafK complexes were affinity purified from nuclear extracts prepared from X63/0 cells expressing eMafK. Mock purification was used as a control. Specific and reproducible bands are indicated with dots.

(B) An immunoblot (IB) analysis of the affinity-purified samples (derived from A) using indicated antibodies. Epitope-tagged and endogenous MafK are shown with dots.

(C) An immunoblot (IB) analysis of the affinity-purified Bach1 complex in MEL cells using indicated antibodies.

(D) Interaction of MafK with MATIIα in Hepa1 cells. Whole-cell extracts of Hepa1 cells (left lanes as an input) were immunoprecipitated with anti-MafK antibody (right lanes) or normal rabbit serum (NRS; middle lanes). The immunoprecipitates were then immunoblotted with indicated antibodies. Short (left) or long (right) exposures are shown.

### Subcellular Localization of MATIIα

To elucidate where MATIIα localizes in a cell, we carried out an immunofluorescence confocal microscopy analysis using X63/0, MEL, and simian virus 40-transformed human fibroblast (GM02063) cells. Individual cells were classified into three

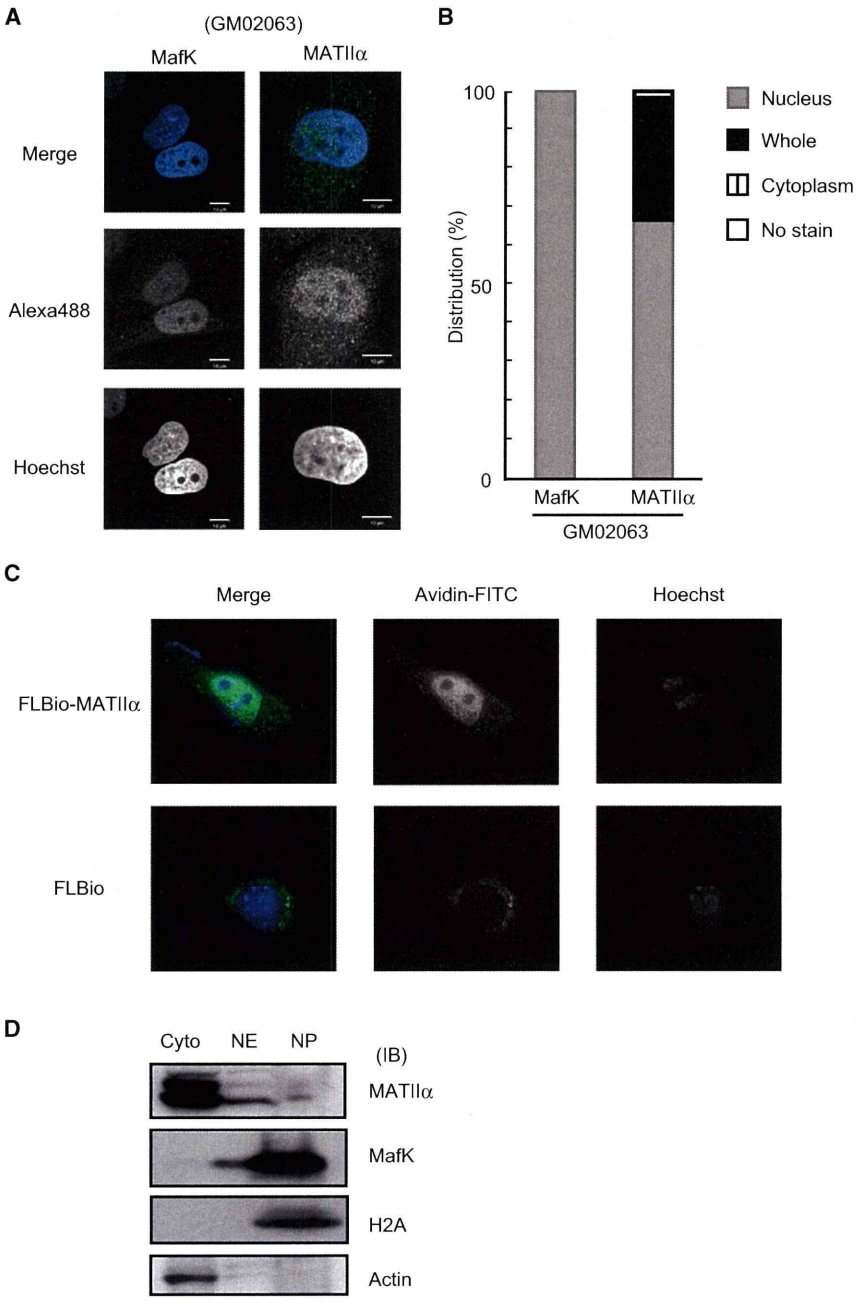


**Figure 2. Subcellular Localization of MafK and MATIIα**

(A) MafK (left) and MATIIα (right) in GM02063 cells were detected by the immunostaining with anti-MafK or MATIIα antibodies. DNA was stained by Hoechst. Merged images show MafK or MATIIα (green) and DNA (blue).

(B) One hundred GM02063 cells stained with anti-MATIIα antibodies were classified into four different categories: nucleus-dominant (gray box), nucleus and cytoplasm (black box), and cytoplasm-dominant (stripe box) staining of MATII.

(C) FLBio-MATIIα (upper panel) was detected with streptavidin-FITC in Hepa1 cells. DNA was stained by Hoechst. Merged images show FLBio-MATIIα (green) and DNA (blue). FLBio plasmid was used as a control (lower panel).

(D) Cytoplasmic (Cyto), nuclear extracts (NE), and nuclear pellet (NP) of MEL cells were analyzed by immunoblotting using indicated antibodies. H2A and actin served as controls for NP and Cyto, respectively.

categories depending on the localization of MATIIα signal: cytoplasmic-dominant, nuclear-dominant, or diffuse distribution. We found that endogenous MATIIα localized in not only cytoplasm but also nucleus of GM02063 (Figures 2A and 2B), X63/0 (Figures S2A and S2C), and MEL (Figures S2B and S2D). As a verification, we next used cells expressing MATIIα tagged with a biotin ligase sequence (FLBio-MATIIα). FLBio-MATIIα or parent FLBio plasmids were transfected in Hepa1 cells together with BirA (biotin-protein ligase). The subcellular localization of MATIIα was detected with streptavidin-conjugated FITC. MATIIα localized predominantly in nucleus (Figure 2C). Upon biochemical fractionation of subcellular compartments of MEL cells, endogenous MATIIα was found in not only cytoplasmic extracts but also nuclear extracts (Figure 2D). A small fraction was found in the insoluble nuclear pellets that contained chromatin including histone H2A. In contrast to the above results, however, more intense MATIIα signal was found in cytoplasmic extracts. While this may be due to leakage during the fractionation procedure, the exact reason is not clear at present. MafK was found mainly in the chromatin fraction (Figure 2D). These results indicated that a fraction of MATIIα was localized in the nuclear compartment of cells.

## Proteomic Analysis of MATIIα-Interacting Proteins

To gain insight into the nuclear function of MATIIα, we purified MATIIα-interacting proteins from nuclear extracts of MEL cells stably coexpressing FLBio-MATIIα and BirA. The expression level of FLBio-MATIIα in MEL cells was similar to that of endogenous MATIIα (Figure S3A). The FLBio-MATIIα biotinylated by BirA was purified from nuclear extracts by biotin-avidin affinity chromatography (Figure 3A, lane 2). As a control, we performed a mock purification from nuclear extracts prepared from MEL cells expressing only BirA (Figure 3A, lane 1). The purified FLBio-MATIIα fraction contained many other proteins at varying stoichiometric ratios.

We employed mass spectrometry to identify the MATIIα-associating proteins. To exclude nonspecific proteins, we also carried out mass spectrometry of the mock samples in parallel.

By comparing two sets of data, there were at least 127 proteins that appeared specific because they were present in three independently purified MATIIα samples but not in three independent samples from mock purification. The complete list of identified proteins is provided as Table S2. The MATIIα-interacting proteins included many proteins with known nuclear functions (Figure 3B). Gene ontology (GO) terms such as transcriptional repression, chromatin assembly and remodeling, and DNA repair and replication were prevalent. The interaction of identified proteins with MATIIα was confirmed by immunoblot analysis (Figure 3C). Among candidate proteins examined, only one protein was not confirmed (data not shown), corroborating the specificity of mass spectrometry analysis. The presence of Bach1 and MafK verified the purification procedure (Figure 3C). The presence of MATIIβ suggested its nuclear function with MATIIα. Some of the interacting proteins belong to the PcG complex (Ring1A, Ring1B, and Yy1), NuRD complex (MTA1, CHD3, CHD4, and RbAp48), Swi/Snf complex (BAF180, BAF155, BAF57, BAF53a, and BAF47), CHRAC complex (ACF1), Sin3 complex (Sin3a), and PARP complex (Supt16/Fact140 and PARP1) (Figures 3B and 3C). To compare MATIIα-interacting proteins with those of MafK under the same condition, we purified MafK from MEL cells using the in vivo biotinylation system and found additional MafK interactors (Figure S3B). Importantly, 13% of these proteins were identified in the MATIIα-interacting proteins (Figures 1A and 3B–3D, Figure S3B, and Tables S1 and S2). These results strongly suggest that MATIIα is involved in the regulation of gene expression by interacting with transcription factors and epigenetic regulators.

## Derepression of HO-1 in MATIIα Knockdown

HO-1, one of the MafK target genes, is repressed by MafK/Bach1 heterodimer that binds to MAREs within the two enhancers (E1 and E2) (Figure 4A). To explore MATIIα function in the regulation of HO-1, we carried out transient knockdown of MATIIα with small interfering RNA (siRNA 604 and 911) in mouse hepatoma (Hepa1) cells. RT-PCR and immunoblotting analyses revealed that MATIIα mRNA and protein remained low for 72 hr after introduction of siRNA (Figures S4A and S4B). Expression of MATI/III, Bach1, β-actin, and α-tubulin (Tuba 4) was not affected by the MATIIα-targeted siRNA (Figures S4A and S4B), confirming the specificity of knockdown. A 3 day (72 hr) incubation with siMATIIα resulted in significant elevation of mRNAs of HO-1 and other MafK target genes, ferritin light-chain, ferroportin, glutathione S-transferase μ1 (GSTμ1), and GSTμ3 (Figure 4B, Figures S4C and S4D). In contrast, ferritin heavy-chain (FTH), NAD(P)H quinone oxidoreductase 1 (NQO1), GSTα4, glutamate-cysteine ligase modifier subunit (GCLM), and glutamate-cysteine ligase catalytic subunit (GCLC) were not affected significantly (Figures S4C and S4D).

The expression of HO-1 was also elevated by treating cells with Bach1 siRNA (siBach1) (Figure S4E), suggesting that MATIIα functioned with MafK-Bach1 heterodimer. Transcription of HO-1 and other MafK target genes is induced in response to diverse stresses including oxidative stress (Keyse and Tyrrell, 1989; Ishii et al., 2000). To determine whether MATIIα was involved in the tuning of inducible expression, we treated Hepa1 cells by adding diethyl maleate (DEM), an oxidative stress inducer, to the culture medium (Figure 4B). Induction of HO-1 was evident in control cells within 4 hr after 100 μM DEM treatment and reached a maximum level by 8 hr (Figure S4F). Upon MATIIα knockdown, HO-1 induction became exaggerated as compared with the control cells (Figure 4B and Figure S4F). It was enhanced upon Bach1 knockdown as well (Figure S4E). Induction of FTL by DEM was also enhanced upon MATIIα knockdown (Figure S4C).

We examined an effect of MATI/III siRNA (siMATI/III) upon expression of MafK target genes and found that expression of HO-1, FTH, FTL, and GSTμ3 was not affected under normal or oxidative conditions (Figures S4G and S4H). Thus, we concluded that the MafK-related function was specific to MATIIα among the isozymes.

## MATIIα Recruitment to the Maf Recognition Element of HO-1 Gene

To further elucidate the nuclear function of MATIIα in terms of MafK complex, we asked whether MATIIα was recruited to the target genes of MafK. We performed chromatin immunoprecipitation (ChIP) assays in X63/0 cells using anti-MAT antibody which recognizes MATIIα and MATI/III, because there is no MATIIα-specific antibody that can be used in a ChIP assay as far as we could determine. Crosslinked chromatin fragments of X63/0 cells were immunoprecipitated using anti-MafK or MAT antibodies, and the two enhancers (E1 and E2) and promoter of HO-1, and the promoter of a neighboring gene Mcm5 were examined and quantified by PCR for relative enrichment (Figures 4C and 4D). MATIIα bound to the E1 enhancer, whereas MafK bound to the three regulatory regions of HO-1.

To further investigate MATIIα binding to HO-1 gene, we utilized FLBio-MATIIα. FLBio-MafK was used as a positive control. Crosslinked chromatin fragments of Hepa1 cells were incubated and pulled down with streptavidin beads (ChPD) (Figures 4E–4I). Among the regions examined, E1 and E2 enhancers of HO-1 were specifically enriched by streptavidin beads from the chromatin of cells expressing biotinylated MATIIα, but not from those expressing BirA alone (Figures 4F–4I, each minus [–] columns). Binding of biotinylated MATIIα, but not of endogenous MATIIα to the HO-1 E2, may reflect differences in the sensitivities of the assays, including epitope accessibilities. Interestingly, the recruitment of biotinylated MATIIα to these enhancers decreased in response to DEM treatment (Figure 4E, right, and Figures 4F–4I, each plus [+] columns), consistent with the repressive function of MATIIα. While we found that biotinylated MafK bound to E1, E2, and promoter of HO-1, binding to the enhancers was higher than the promoter (Figures 4F–4H). This may suggest that the specific recruitment of biotinylated MATIIα to E1 and E2 was mediated by MafK. These results indicate that not only MafK but also MATIIα bound specifically to the HO-1 gene and suggest a specific role for MATIIα in transcription regulation. In addition, departure of MATIIα upon oxidative stress may be a critical step for the HO-1 induction.

## Modification of Histone H3 at the HO-1 Locus

Considering the fact that MATIIα synthesizes SAM required for histone and DNA methylation, we hypothesized that knockdown of MATIIα affected repressive methylation at the HO-1 chromatin

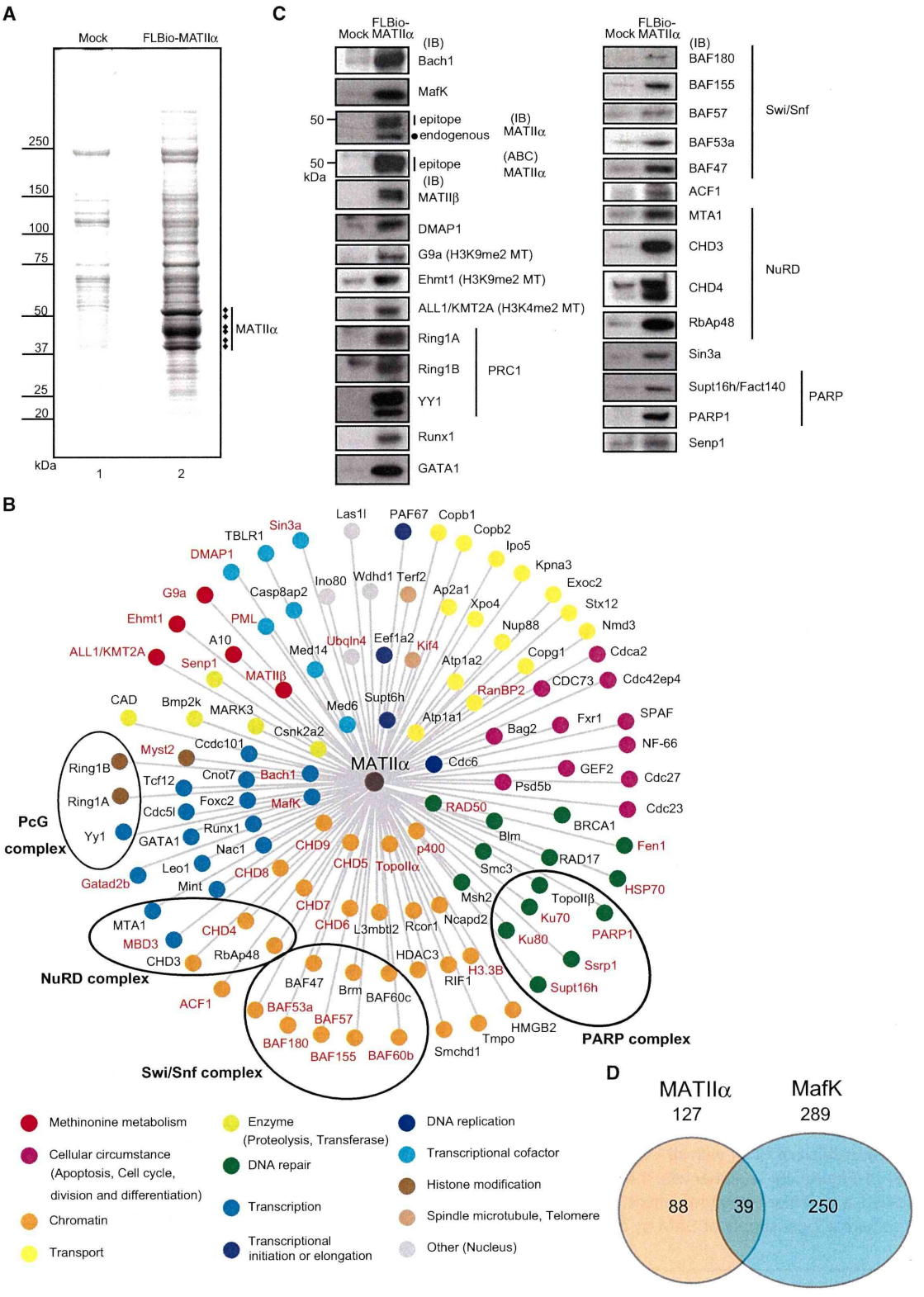


**Figure 3. Purification of MATIIα-Associating Proteins**

(A) MATIIα was affinity purified from MEL cells stably coexpressing FLBio-MATIIα and BirA. Purification from cells expressing only BirA (mock) was used as a control. MATIIα bands are indicated with dots.

domain. To investigate this possibility, we examined the degree of repressive modification (i.e., trimethyl and dimethyl K9 [H3K9 me3 and me2] and trimethyl K27 [H3K27 me3]) and activating modifications (i.e., dimethyl K4 [H3K4 me2], acetyl K9 [H3K9 Ac], acetyl K27 [H3K27 Ac], and trimethyl K36 [H3K36 me3]) of histone H3 at HO-1 locus using ChIP (Figures 5A–5C). There was no detectable level of H3 K9 and K27 me3 at the HO-1 locus (Figure 5A). In contrast, H3K9 me2 was clearly observed at the E1 region (Figure 5C). As previously reported for NIH 3T3 cells (Sun et al., 2004), histone H3K4 at the enhancers (E1 and E2) and promoter of HO-1 was hypermethylated under normal culture condition (Figure 5A). Upon MATIIα knockdown, H3K4 me2 and H3K9 me2 decreased (Figures 5A–5C). H3K36 me3, linked to transcriptional elongation, was detected at the exon 3 region of HO-1 in both control and MATIIα knockdown cells (Figure 5A). There are CpG islands in the E2 and promoter regions of HO-1 (data not shown). We examined CpG methylation in these regions by bisulphite genomic sequencing. The E2 and promoter regions of HO-1 were found devoid of CpG methylation under normal conditions (Figure S5A). Taken together with a recent report that H3K4 me2 recruits the Set3 histone deacetylase complex to suppress nucleosome acetylation and remodeling (Kim and Buratowski, 2009), these observations suggest that the repression of HO-1 by MATIIα may involve the H3K4 me2 and H3K9 me2 marks.

## Catalytic Activity of MATIIα Involved in the Repression of HO-1

To investigate whether the catalytic activity of MATIIα is required to repress HO-1, we constructed a mutated MATIIα (MATIIα D134A) converting aspartic acid of amino acid 134 to alanine. MAT enzymes possess an evolutionary conserved common ATP binding motif (GXGDXG) (Figure S5B). A mutation of the aspartic acid within this motif of human MATI/III almost completely abolishes the catalytic activity (Chamberlin et al., 2000, and Figure S5B). We treated Hepa1 cells expressing wild-type MATIIα or MATIIα D134A by adding DEM and compared the relative expression of HO-1 with control cells (Figure 5D). Upon overexpression of MATIIα D134A, induction of HO-1 mRNA became exaggerated as compared with the control cells (Figure 5D). Overexpression of wild-type MATIIα did not show such a stimulatory effect (Figure 5D). These data indicated that the enzymatic activity of MATIIα was required for the repression of HO-1 by MafK and Bach1.

The dominant-negative effect of MATIIα D134A upon HO-1 regulation suggested that a simple lack of SAM was not the cause of HO-1 derepression upon MATIIα knockdown. To test this idea, we treated cells with both siMATIIα and ectopic SAM. The derepression of HO-1 with siMATIIα was not reversed by adding SAM (Figure 5E). Together with the results that MATIIα D134A showed a dominant-negative effect, the repression of HO-1 may require a local supply of SAM by MATIIα.

## MATIIα-Associating Factors Involved in the Repression of HO-1

Among the MATIIα-associating proteins (Figure 3), we chose several proteins that were known to play roles in gene repression and MATIIβ to investigate their involvement in HO-1 repression. BAF53a, CHD4, or MATIIβ knockdown (siBAF53a, siCHD4, or siMATIIβ) resulted in derepression of HO-1 under normal conditions (Figure 6A and Figures S6A and S6B). E1 and E2 enhancers and promoter of HO-1 were specifically enriched by anti-BAF53a, anti-CHD4, or anti-MATIIβ antibodies (Figure 6B), showing their binding to the HO-1 regulatory regions. Recruitment of BAF53a and CHD4 to the HO-1 locus was not abolished upon MATIIα knockdown (Figure S6C), indicating that MATIIα was not required for their recruitment. PARP1 knockdown also resulted in HO-1 derepression under the presence of oxidative stress (Figure 6C and Figures S6A and S6B).

## Association of Methyltransferase Activity with MATIIα

The involvement of both the catalytic activity of MATIIα and its interacting factors in the HO-1 repression suggested that these factors might further interact with methyltransferases. To investigate this possibility, methyltransferase activity associated with MATIIα was determined by a conventional histone methyltransferase (HMT) assay. Recombinant G9a and FLBio-MATIIα fraction affinity purified from MEL cells using avidin beads showed methylation activities toward histone H1 and H3, whereas the corresponding fraction purified from control cell (mock) contained significantly less activity (Figures 7A–7C).

The copurification of MATIIα and HMT activities suggested that SAM synthesis and methylation might be coupled by their physical interaction. To investigate this possibility, we developed a new HMT assay involving synthesis of SAM from methionine and ATP (MAT-HMT assay). The affinity-purified FLBio-MATIIα fraction, without any extraneous methyltransferase added, showed methylation activity toward histone H1 and H3, and this activity was dependent on ATP (Figures 7D–7F). In contrast, recombinant G9a and mock fraction did not modify histones (Figure 7D). These results strongly suggested that MATIIα associated with histone H1 and H3 methyltransferases in the nuclei.

To characterize the relationship among MATIIα, MATIIβ, BAF53a, CHD4, PARP1, and HMT activities, we obtained MATIIα-enriched materials by single anti-FLAG affinity purification of biotinylated FLBio-MATIIα from MEL cells, and fractionated them using 10%–35% (v/v) glycerol gradient sedimentation. Whereas MATIIα and β subunits formed peaks corresponding to around 158 kDa, substantial portions of them sedimented much faster, indicating the presence of a high-molecular-mass form of roughly 640 kDa (Figure 7G). MATIIα may form several different complexes, or associations of the complex components may be fragile. BAF53a, CHD4, Bach1, and MafK were found in the relatively faster-sedimenting fractions (Figure 7G). PARP1 presumably modified by poly-ADP-ribosylation was also present

(B) MATIIα-associated proteins were categorized by gene ontology (GO) annotations as listed in the *Mus musculus* Genome Database. Known protein complexes are denoted by black circles. Proteins found in the MafK complex (Figure S4) are shown in red. Those found in the MafK complex in Figure 1 are shown in bold.
(C) Immunoblot (IB) analysis of the affinity-purified samples (derived from A) using indicated antibodies or by a biotin-avidin complex (ABC) analysis (FLBio-MATIIα).
(D) Venn diagram of proteins associated with FLBio-MATIIα or FLBio-MafK in MEL cells.

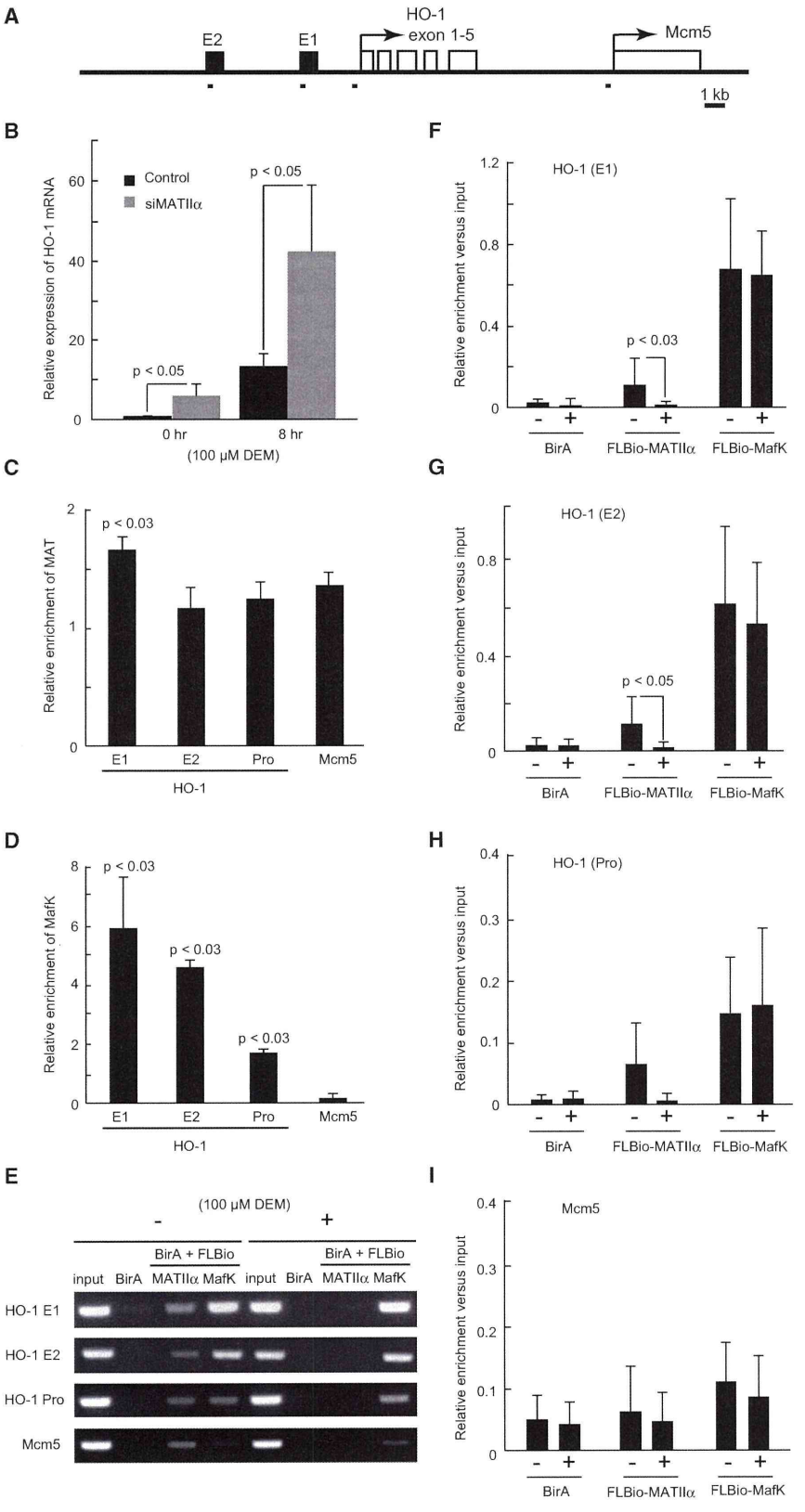


**Figure 4. MATIIα Recruitment to HO-1 Locus**

(A) Schematic representation of mouse HO-1 and Mcm5 loci. Lines below indicate PCR primer pairs for ChIP and ChPD analyses.

(B) Quantitative RT-PCR (qRT-PCR) analysis of HO-1 mRNA in Hepa1 cells with control (black) and MATIIα siRNA (gray). Cells were treated with or without 100 μM DEM for 8 hr. The expression level of HO-1 gene in control under normal condition was arbitrarily set at 1. β-actin mRNA measurement was used to normalize the results. The averages of three independent experiments with standard deviation are shown. P values (Student's t test) for differences between control and MATIIα siRNA are indicated.

(C and D) ChIP assays were performed by using antibodies to MAT (C) or MafK (D) with X63/0 cells. Relative levels of enrichment of each genomic DNA region compared to control IgG are shown. These results represent three independent experiments with standard deviation. P values (Student's t test) for differences between MAT (C) or MafK (D) and control rabbit IgG signals are indicated.

(E) ChPD assays were performed with Hepa1 cells coexpressing FLBio-MATIIα or FLBio-MafK and BirA. Cells expressing only BirA were examined as a control. Cells were treated with or without 100 μM DEM for 8 hr. Gel images of PCR products of indicated regions are shown.

(F–I) ChPD assays were performed as above and quantified. Relative levels of enrichment of the indicated genomic regions are shown. These results represent three independent experiments with standard deviation. P values (Mann-Whitney U test) for differences between cells treated with or without DEM are indicated.

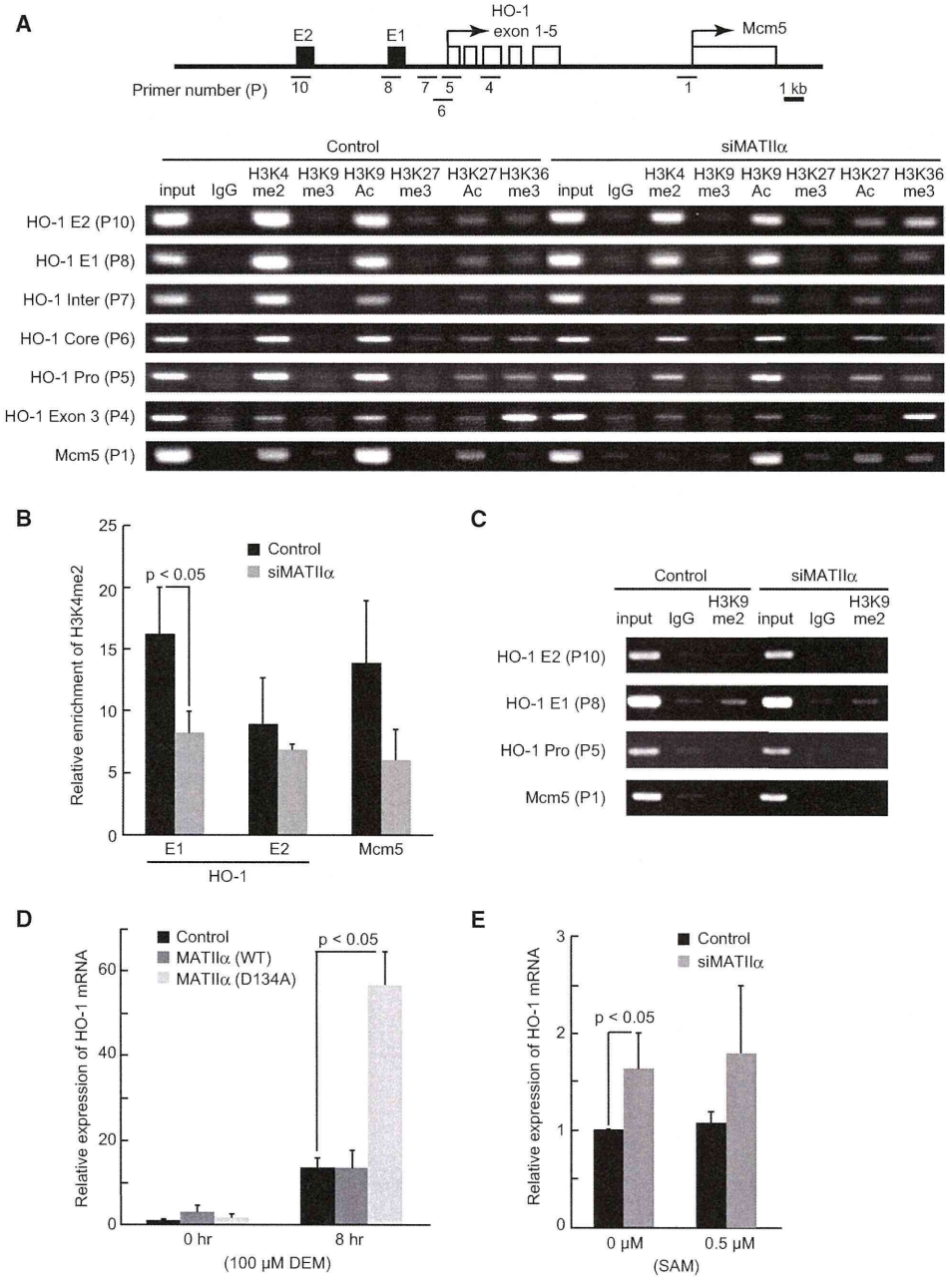


**Figure 5. Enzymatic Activity of MATIIα and Repression of HO-1**

(A) Schematic representation of mouse HO-1 and Mcm5 loci (upper). Primers used to amplify various genomic regions are also shown. Cells were treated with control or MATIIα siRNA, and ChIP assays were performed using indicated antibodies (lower).

(B) Relative levels of dimethylated histone H3 (K4 me2) at indicated genomic regions in Hepa1 cells treated with control (black) or MATIIα siRNA (gray). The averages of three independent experiments with standard deviation are shown. P value (Student's t test) for differences is indicated.

(C) Dimethylated H3K9 at HO-1 locus. ChIP assays were performed as in (A) using dimethylated histone H3 (K9 me2) antibody.

(D) qRT-PCR analysis of HO-1 mRNA in control cells (black) or those overexpressing wild-type MATIIα (gray) or MATIIα D134A (light gray). These cells were treated with DEM for 8 hr. The averages of three independent experiments with standard deviation are shown. The expression level of HO-1 gene in control under normal condition was arbitrarily set at 1. β-actin mRNA measurement was used to normalize the results.

(E) qRT-PCR analysis of HO-1 mRNA in cells treated with control (black) or MATIIα siRNA (gray). Cells were treated with or without 0.5 μM SAM for 12 hr.

in these fractions. We pooled respective fractions to compare the smaller and larger MATIIα fractions in detail (S1 and S2 in Figure 7G) and carried out further purification using biotin-avidin affinity chromatography (Figure 7H). Whereas BAF53a, Bach1, and MafK interacted with MATIIα in both fractions, interaction of CHD4 was found mainly in the larger fractions (Figure 7H).

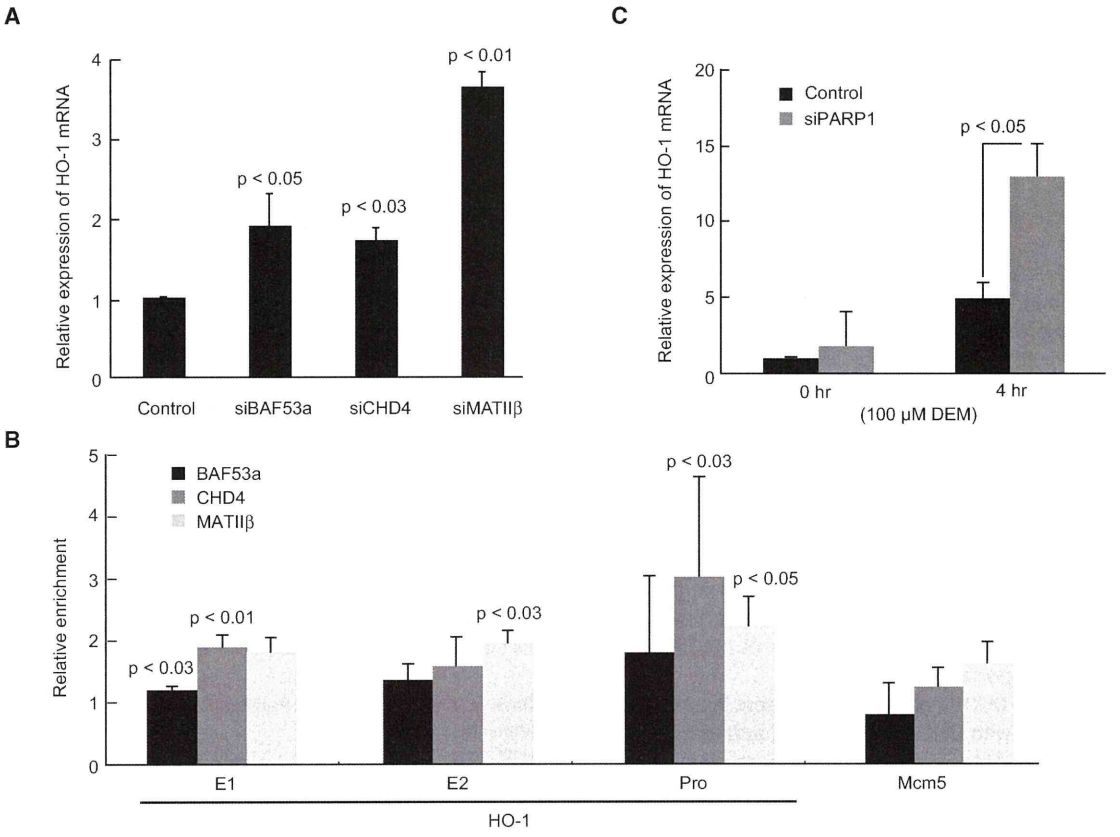


**Figure 6. MATII-Associating Factors Repress HO-1 Expression**

(A) qRT-PCR analysis of HO-1 mRNA in Hepa1 cells treated with control, siBAF53a, siCHD4, or siMATIIβ. Error bars represent standard deviation.

(B) BAF53a, CHD4, and MATIIβ were recruited to HO-1 locus. ChIP assays were performed using indicated antibodies. Relative levels of enrichment of indicated genomic DNA regions are shown with standard deviation. P values (Student's t test) for differences between specific antibodies and control rabbit IgG signals are indicated.

(C) qRT-PCR analysis of HO-1 in cells treated with control (black) or PARP1 siRNA (gray). Cells were treated with or without 100 μM DEM for 4 hr.

Interaction of PARP1 was hardly detected in either fraction (data not shown), suggesting that its interaction with MATIIα was labile and lost. The two forms of MATIIα were examined for SAM synthesis and histone methylation in MAT-HMT assay (Figure 7I). We found that only the high-molecular-mass form of MATIIα and its interacting proteins purified from the larger fractions showed SAM synthesis-dependent methylation activity toward histone H1 and H3 (Figure 7I). These results suggest that biosynthesis of SAM is physically coupled with histone methylation on chromatin (Figure 7J).

## DISCUSSION

While SAM is essential for histone and DNA methylation, little is known about the function of MATIIα in the context of gene and chromatin regulation. A previous report identified MATIIα as a modifier mutation of chromatin architecture (Larsson et al., 1996). In *Drosophila melanogaster*, modifier mutations of position-effect variegation and PcG genes have been useful tools to investigate genes involved in chromatin architecture. Suppressor of zeste 5 (Su[z]5) encodes MATIIα and acts as enhancers of Polycomb (i.e., reduced activity of both MATIIα and Polycomb resulting in chromatin derepression), suggesting that MATIIα is involved in the process of gene silencing in fly (Larsson et al., 1996). However, this historical study has not been followed up as far as we know, and mechanistic defects in the Su(z)5 mutant are not known. We have extended this study and revealed the molecular function of MATIIα by proteomics analyses of MafK, Bach1, and MATIIα (Figures 1 and 3).

We showed that a fraction of MATIIα was localized in the nuclear compartment of various cells (Figure 2). We also found that MATIIα was recruited to MARE of enhancers at HO-1 locus in X63/0 and Hepa1 cells (Figures 4C and 4E–4I). Upon MATIIα knockdown, mRNA and protein levels of HO-1 were elevated and further induced strongly upon DEM treatment (Figure 4B and data not shown). MATIIα knockdown showed similar effects upon some other MafK target genes (Figures S4C and S4D). These observations suggest collectively that MATIIα functions as a corepressor of MafK and Bach1.

The purification of MATIIα from MEL cells provided strong evidences for its functions around chromatin. MATIIα was

copurified along with proteins with known chromatin and epigenetic functions (Figure 3). Among them were PARP1 and components of NuRD, Swi/Snf-like BAF, and PcG complexes (Figure 3B). Indeed, knockdown of PARP1, BAF53a (Swi/Snf-like BAF complex), and CHD4 (NuRD complex) resulted in derepression of HO-1 (Figures 6A and 6C). Since these proteins are known to repress the expression of target genes as corepressors of transcription and/or remodeling factors of chromatin architecture (Brand et al., 2004, Wacker et al., 2007), these proteins, together with MATIIα, may also participate in target gene repression by MafK and Bach1 (Figure 7J).

MATIIβ is known to inhibit the catalytic activity of MATIIα by sensitizing it to the product inhibition by SAM (LeGros et al., 2001). We found that MATIIβ was recruited to the MafK target genes and required for their repression, indicating that MATIIβ is a stimulatory rather than inhibitory subunit of MATIIα in terms of transcription regulation. Recently, it has been reported that splicing variants of MATIIβ are present in nuclei and interact with mRNA binding protein HuR (Xia et al., 2010). Although its relevance to transcription regulation is not clear at present and we did not detect HuR in our proteomics analyses, this finding also supports nuclear function of MATIIβ. Since β-like subunit is not found in MATI/III, molecular function of MATIIβ on chromatin will be an important issue.

Considering that MATIIα and -β were present in a high-molecular-mass fraction with CHD4 and BAF53a, and that this particular form coupled SAM synthesis and histone methylation in vitro (Figure 7I), the core of this form, MATIIα and MATIIβ, was named the SAMIT module. "Module" is used to reflect our observations that MATIIβ was also critical for the corepressor activity and that they further interacted with chromatin regulators and histone H1 and H3 methyltransferase activities (Figure 7J). The interaction of methyltransferase activities with SAMIT module suggests that SAM produced by MATIIα in situ may be utilized to inhibit MafK/Bach1 target genes. Whereas the catalytically inactive MATIIα interfered with HO-1 repression, exogenous SAM failed to reverse the effect of MATIIα knockdown (Figures 5D and 5E). These observations support the notion that the catalytic function of MATIIα plays a role at sites of recruitment. SAM may be utilized for methylation of protein(s) (Figure 7J). One possible target may be dimethylation of H3K4 and K9, which can potentially inhibit transcription via regulation of histone acetylation and remodeling on euchromatic regions (Figures 5A–5C; Kim and Buratowski, 2009; Fritsch et al., 2010). While we identified G9a, Ehmt1, and ALL1/KMT2A methyltransferases upon the single-step purification of MATIIα (Figure 3), we did not detect them in the further purified SAMIT module (Figure 7H) by immunoblotting analysis (data not shown). Thus, the interaction of MATIIα with G9a and ALL1 may be dynamic. Identification of the methyltransferase activities copurified with SAMIT is now underway.

The list of MATIIα-associated proteins suggests functions of MATIIα and SAMIT beyond MafK. The presence of DNA-binding transcription factors such as GATA1 and Runx1 in the MATII-associating proteins (Figure 3) raises the possibility that these transcription factors may utilize MATIIα/SAMIT as a coregulator as well. Several Polycomb-related proteins were found in the purified MATIIα fraction, being consistent with the genetic interaction with Polycomb in *Drosophila melanogaster* (Larsson et al., 1996).

Regulation of metabolic flux by enzyme compartmentalization is a well-established concept. The presence of MATIIα in nuclear compartment may allow efficient coupling of SAM synthesis and methylation of target protein or DNA by methyltransferases. Considering that SAM is an energetically precious but labile molecule generated in the expense of ATP, its production in situ may allow fine and efficient tuning of the cascade reactions for histone and DNA methylation. The list of MATIIα-associating proteins will be helpful to foster integrative understanding of chromatin-based regulations.

## EXPERIMENTAL PROCEDURES

### Plasmids

pOZ-N-MafK plasmid was described previously (Ochiai et al., 2006). Construction of MATIIα expression plasmid is described in the Supplemental Experimental Procedures.

### Immunohistochemistry

Basic indirect immunofluorescence of paraformaldehyde-fixed cells was described previously (Francastel et al., 2001). All processes are described in the Supplemental Experimental Procedures.

### MafK and MATIIα Complex Purification and Mass Spectrometric Analysis

MafK complex purification was carried out as previously described from X63/0 cells expressing eMafK (Ochiai et al., 2006). FLBio-tagged protein purification was carried out as previously described (de Boer et al., 2003). Each protein was determined using LC-HCT plus (Bruker Daltonics) or LTQ (Thermo Fisher Scientific), and MASCOT search engine (Matrix Science). Glycerol gradient sedimentation was carried out as previously described (Dohi et al., 2008) and also described in the Supplemental Experimental Procedures.

### RNA Interference

Stealth RNAi duplexes were designed to target MATIIα and β, MafK, BAF53a, CHD4, and PARP1 using the BLOCK-iT RNAi Designer (Invitrogen Corporation, Carlsbad, CA). All RNAi sequences are described in the Supplemental Experimental Procedures.

### ChIP and ChPD Analysis

ChIP and ChPD were performed as described previously (Sawado et al., 2001; de Boer et al., 2003). Anti-methylated H3K4 and H3K9, and anti-acetylated H3K9 and H3K27 antibodies were described previously (Kimura et al., 2008). The enrichment of the DNA template was analyzed and quantified by semi-quantitive PCR using primers as described in the Supplemental Experimental Procedures. Relative enrichment was calculated as the difference between specific antibody and normal IgG signals (ChIP), or as that of FLBio-MATIIα or FLBio-MafK and BirA signals (ChPD) normalized to the respective input signals.

### In Vitro HMT and MAT-HMT Assay

In vitro HMT assays were performed as described previously (Tachibana et al., 2001). In vitro MAT-dependent HMT (MAT-HMT) assays were carried out by modifying in vitro HMT assay. All processes are described in the Supplemental Experimental Procedures.

## SUPPLEMENTAL INFORMATION

Supplemental Information includes Supplemental Experimental Procedures, Supplemental References, six figures, and two tables and can be found with this article at doi:10.1016/j.molcel.2011.02.018.

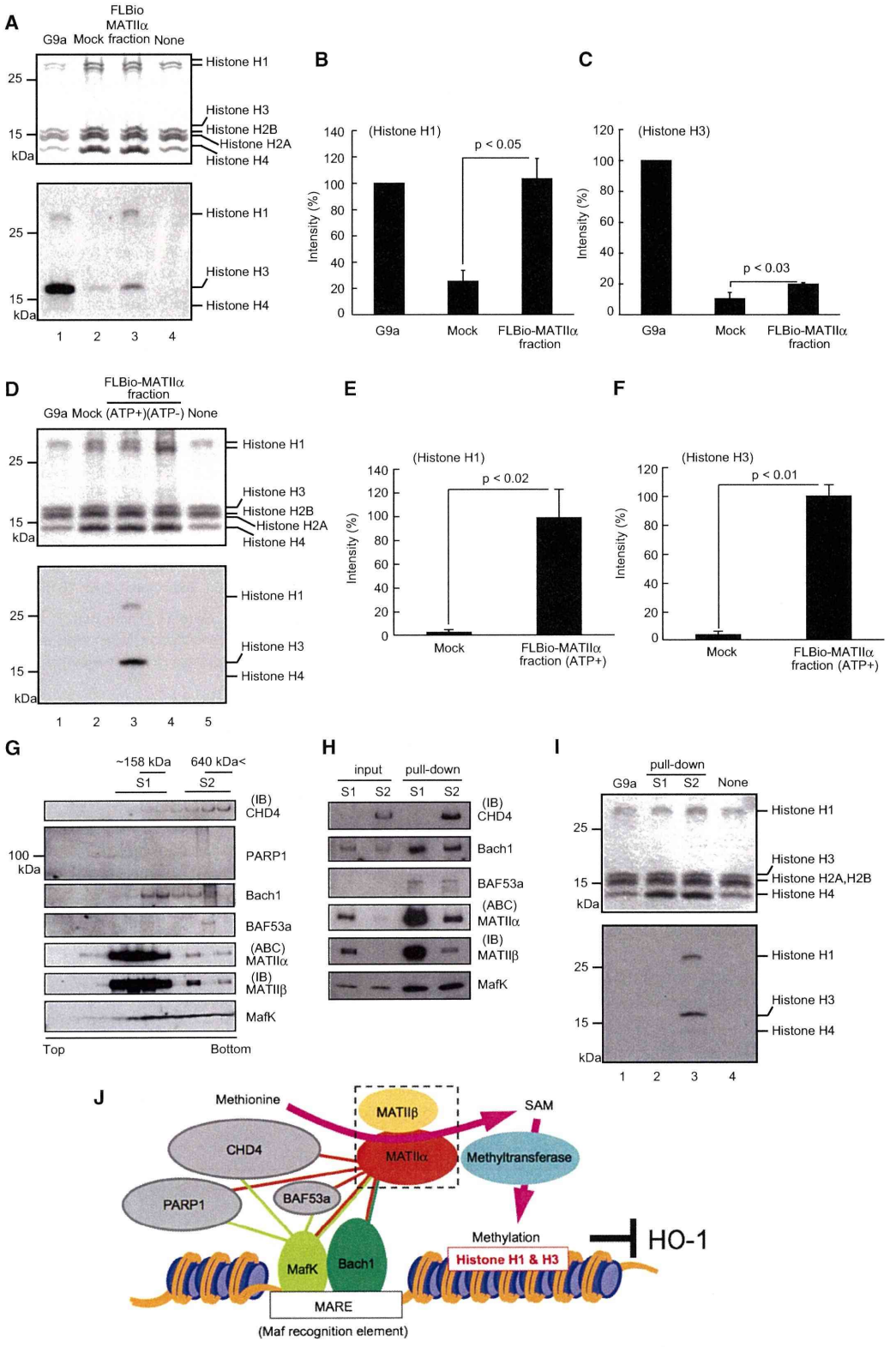


**Figure 7. Interaction of Methyltransferase Activity with MATIIα**

(A) HMT assays were carried out with recombinant GST-G9a (lane 1), affinity-purified fractions of control cells (mock; lane 2) or MATIIα cells (FLBio-MATIIα; lane 3) using avidin beads, or no protein added (none; lane 4). CBB staining (top panel) and fluorography (bottom panel) are shown.

## ACKNOWLEDGMENTS

We thank Dr. H. Motohashi (Tohoku University) for critical reading of the manuscript and comments; C. Teruya (Tohoku University) for mass spectrometric analysis; Drs. K. Itoh, A. Maruyama (Hirosaki University), J. Sharif, Y. Dohi, A. Muto, K. Murayama (Tohoku University), and M. Matsumoto and K. Nakayama (Kyusyu University) for discussion and help; Dr. H. Kimura (Osaka University) for antibodies to methylated H3K4 and H3K9, and acetylated H3K9 and H3K27; and Dr. M. Tachibana (Kyoto University) for HMT assay protocol. The biotin tag system was kindly provided by Dr. A.B. Cantor (Children's Hospital Boston). This work was supported by Grants-in-aid from the Ministry of Education, Science, Sport, and Culture of Japan, grant from the Naito Foundation for Research on "Nuclear Dynamics and RNA," grant from the Nukada scholarship, Toho University, and global COE program for Network Medicine, Tohoku University. Part of this study was supported by Biomedical Research Core of Tohoku University School of Medicine.

Received: November 6, 2009
Revised: August 18, 2010
Accepted: December 22, 2010
Published: March 3, 2011

## REFERENCES

Andrews, N.C., Erdjument-Bromage, H., Davidson, M.B., Tempst, P., and Orkin, S.H. (1993). Erythroid transcription factor NF-E2 is a haematopoietic-specific basic-leucine zipper protein. Nature *362*, 722–728.

Brand, M., Ranish, J.A., Kummer, N.T., Hamilton, J., Igarashi, K., Francastel, C., Chi, T.H., Crabtree, G.R., Aebersold, R., and Groudine, M. (2004). Dynamic changes in transcription factor complexes during erythroid differentiation revealed by quantitative proteomics. Nat. Struct. Mol. Biol. *11*, 73–80.

Chamberlin, M.E., Ubagai, T., Pao, V.Y., Pearlstein, R.A., and Chou, J.Y. (2000). Structural requirements for catalysis and dimerization of human methionine adenosyltransferase I/III. Arch. Biochem. Biophys. *373*, 56–62.

de Boer, E., Rodriguez, P., Bonte, E., Krijgsveld, J., Katsantoni, E., Heck, A., Grosveld, F., and Strouboulis, J. (2003). Efficient biotinylation and single-step purification of tagged transcription factors in mammalian cells and transgenic mice. Proc. Natl. Acad. Sci. USA *100*, 7480–7485.

Dillon, S.C., Zhang, X., Trievel, R.C., and Cheng, X. (2005). The SET-domain protein superfamily: protein lysine methyltransferases. Genome Biol. *6*, 227.

Dohi, Y., Ikura, T., Hoshikawa, Y., Katoh, Y., Ota, K., Nakanome, A., Muto, A., Omura, S., Ohta, T., Ito, A., et al. (2008). Bach1 inhibits oxidative stress-induced cellular senescence by impeding p53 function on chromatin. Nat. Struct. Mol. Biol. *15*, 1246–1254.

Francastel, C., Magis, W., and Groudine, M. (2001). Nuclear relocation of a transactivator subunit precedes target gene activation. Proc. Natl. Acad. Sci. USA *98*, 12120–12125.

Fritsch, L., Robin, P., Mathieu, J.R., Souidi, M., Hinaux, H., Rougeulle, C., Harel-Bellan, A., Ameyar-Zazoua, M., and Ait-Si-Ali, S. (2010). A subset of the histone H3 lysine 9 methyltransferases Suv39h1, G9a, GLP, and SETDB1 participate in a multimeric complex. Mol. Cell *37*, 46–56.

Fujiwara, K.T., Kataoka, K., and Nishizawa, M. (1993). Two new members of the maf oncogene family, mafK and mafF, encode nuclear b-Zip proteins lacking putative trans-activator domain. Oncogene *8*, 2371–2380.

Goll, M.G., and Bestor, T.H. (2005). Eukaryotic cytosine methyltransferases. Annu. Rev. Biochem. *74*, 481–514.

Halim, A.B., LeGros, L., Chamberlin, M.E., Geller, A., and Kotb, M. (2001). Regulation of the human MAT2A gene encoding the catalytic alpha 2 subunit of methionine adenosyltransferase, MAT II: gene organization, promoter characterization, and identification of a site in the proximal promoter that is essential for its activity. J. Biol. Chem. *276*, 9784–9791.

Hall, D.A., Zhu, X., Royce, T., Gerstein, M., and Snyder, M. (2004). Regulation of gene expression by a metabolic enzyme. Science *306*, 482–484.

Hintze, K.J., Katoh, Y., Igarashi, K., and Theil, E.C. (2007). Bach1 repression of ferritin and thioredoxin reductase1 is heme-sensitive in cells and in vitro and coordinates expression with heme oxygenase1, beta-globin, and NADP(H) quinone (oxido) reductase1. J. Biol. Chem. *282*, 34365–34371.

Igarashi, K., and Sun, J. (2006). The heme-Bach1 pathway in the regulation of oxidative stress response and erythroid differentiation. Antioxid. Redox Signal. *8*, 107–118.

Igarashi, K., Kataoka, K., Itoh, K., Hayashi, N., Nishizawa, M., and Yamamoto, M. (1994). Regulation of transcription by dimerization of erythroid factor NF-E2 p45 with small Maf proteins. Nature *367*, 568–572.

Igarashi, K., Itoh, K., Motohashi, H., Hayashi, N., Matuzaki, Y., Nakauchi, H., Nishizawa, M., and Yamamoto, M. (1995). Activity and expression of murine small Maf family protein MafK. J. Biol. Chem. *270*, 7615–7624.

Ishii, T., Itoh, K., Takahashi, S., Sato, H., Yanagawa, T., Katoh, Y., Bannai, S., and Yamamoto, M. (2000). Transcription factor Nrf2 coordinately regulates a group of oxidative stress-inducible genes in macrophages. J. Biol. Chem. *275*, 16023–16029.

Itoh, K., Chiba, T., Takahashi, S., Ishii, T., Igarashi, K., Katoh, Y., Oyake, T., Hayashi, N., Satoh, K., Hatayama, I., et al. (1997). An Nrf2/small Maf heterodimer mediates the induction of phase II detoxifying enzyme genes through antioxidant response elements. Biochem. Biophys. Res. Commun. *236*, 313–322.

Kataoka, K., Igarashi, K., Itoh, K., Fujiwara, K.T., Noda, M., Yamamoto, M., and Nishizawa, M. (1995). Small Maf proteins heterodimerize with Fos and may act as competitive repressors of the NF-E2 transcription factor. Mol. Cell. Biol. *15*, 2180–2190.

Keyse, S.M., and Tyrrell, R.M. (1989). Heme oxygenase is the major 32-kDa stress protein induced in human skin fibroblasts by UVA radiation, hydrogen peroxide, and sodium arsenite. Proc. Natl. Acad. Sci. USA *86*, 99–103.

Kim, T., and Buratowski, S. (2009). Dimethylation of H3K4 by Set1 recruits the Set3 histone deacetylase complex to 5′ transcribed regions. Cell *137*, 259–272.

Kimura, H., Hayashi-Takanaka, Y., Goto, Y., Takizawa, N., and Nozaki, N. (2008). The organization of histone H3 modifications as revealed by a panel of specific monoclonal antibodies. Cell Struct. Funct. *33*, 61–73.

(B and C) Relative levels of methylation of histone H1 (B) and H3 (C) are shown. The methylation level of histones by GST-G9a was arbitrarily set at 100%. These results represent three independent experiments with standard deviation.
(D) MAT-HMT assays were carried out using ATP and labeled methionine as in (A). ATP was omitted in lane 4.
(E and F) Relative levels of methylation of histone H1 (E) and H3 (F) in (D) are shown. The methylation level of histones by MATIIα fraction was arbitrarily set at 100%. These results represent three independent experiments with standard deviation.
(G–I) FLBio-MATIIα was purified using FLAG antibody and then separated with glycerol gradient centrifugation. Fractions were analyzed with indicated antibodies (G). FLBio-MATIIα was further affinity purified from the pooled fractions (S1 and S2 in G) using biotin-avidin and analyzed as above (H). MAT-HMT assay with recombinant GST-G9a or the purified MATIIα complex from S1 or S2 were carried out (I). Reaction mixtures alone were used as a control (none; lane 4). CBB-stained gel (top) and fluorography (bottom) are shown, representing three independent studies.
(J) A model for MATII function. Copurified proteins are connected with lines whose colors indicate tagged bait proteins. MATIIα functions as a corepressor of MafK-Bach1 by locally providing SAM and forming SAMIT module with MATIIβ (dashed line). SAM may be used for methylation required for repression including histone H1 and H3 such as H3K4 and K9 me2.

Kotb, M., Mudd, S.H., Mato, J.M., Geller, A.M., Kredich, N.M., Chou, J.Y., and Cantoni, G.L. (1997). Consensus nomenclature for the mammalian methionine adenosyltransferase genes and gene products. Trends Genet. *13*, 51–52.

Larsson, J., Zhang, J., and Rasmuson-Lestander, A. (1996). Mutations in the Drosophila melanogaster gene encoding S-adenosylmethionine synthetase suppress position-effect variegation. Genetics *143*, 887–896.

LeGros, L., Halim, A.B., Chamberlin, M.E., Geller, A., and Kotb, M. (2001). Regulation of the human MAT2B gene encoding the regulatory beta subunit of methionine adenosyltransferase, MAT II. J. Biol. Chem. *276*, 24918–24924.

Lu, S.C., and Mato, J.M. (2008). S-Adenosylmethionine in cell growth, apoptosis and liver cancer. J. Gastroenterol. Hepatol. *23* (*Suppl 1*), S73–S77.

Motohashi, H., Katsuoka, F., Shavit, J.A., Engel, J.D., and Yamamoto, M. (2000). Positive or negative MARE-dependent transcriptional regulation is determined by the abundance of small Maf proteins. Cell *103*, 865–875.

Muto, A., Hoshino, H., Madisen, L., Yanai, N., Obinata, M., Karasuyama, H., Hayashi, N., Nakauchi, H., Yamamoto, M., Groudine, M., and Igarashi, K. (1998). Identification of Bach2 as a B-cell-specific partner for small maf proteins that negatively regulate the immunoglobulin heavy chain gene 3′ enhancer. EMBO J. *17*, 5734–5743.

Muto, A., Tashiro, S., Nakajima, O., Hoshino, H., Takahashi, S., Sakoda, E., Ikebe, D., Yamamoto, M., and Igarashi, K. (2004). The transcriptional programme of antibody class switching involves the repressor Bach2. Nature *429*, 566–571.

Ochiai, K., Katoh, Y., Ikura, T., Hoshikawa, Y., Noda, T., Karasuyama, H., Tashiro, S., Muto, A., and Igarashi, K. (2006). Plasmacytic transcription factor Blimp-1 is repressed by Bach2 in B cells. J. Biol. Chem. *281*, 38226–38234.

Ochiai, K., Muto, A., Tanaka, H., Takahashi, S., and Igarashi, K. (2008). Regulation of the plasma cell transcription factor Blimp-1 gene by Bach2 and Bcl6. Int. Immunol. *20*, 453–460.

Oyake, T., Itoh, K., Motohashi, H., Hayashi, N., Hoshino, H., Nishizawa, M., Yamamoto, M., and Igarashi, K. (1996). Bach proteins belong to a novel family of BTB-basic leucine zipper transcription factors that interact with MafK and regulate transcription through the NF-E2 site. Mol. Cell. Biol. *16*, 6083–6095.

Reytor, E., Pérez-Miguelsanz, J., Alvarez, L., Pérez-Sala, D., and Pajares, M.A. (2009). Conformational signals in the C-terminal domain of methionine adenosyltransferase I/III determine its nucleocytoplasmic distribution. FASEB J. *23*, 3347–3360.

Sakata, S.F., Shelly, L.L., Ruppert, S., Schutz, G., and Chou, J.Y. (1993). Cloning and expression of murine S-adenosylmethionine synthetase. J. Biol. Chem. *268*, 13978–13986.

Sakata, S.F., Okumura, S., Matsuda, K., Horikawa, Y., Maeda, M., Kawasaki, K., Chou, J.Y., and Tamaki, N. (2005). Effect of fasting on methionine adenosyltransferase expression and the methionine cycle in the mouse liver. J. Nutr. Sci. Vitaminol. (Tokyo) *51*, 118–123.

Sawado, T., Igarashi, K., and Groudine, M. (2001). Activation of β-major globin gene transcription is associated with recruitment of NF-E2 to the β-globin LCR and gene promoter. Proc. Natl. Acad. Sci. USA *98*, 10226–10231.

Shi, Y. (2007). Histone lysine demethylases: emerging roles in development, physiology and disease. Nat. Rev. Genet. *8*, 829–833.

Sun, J., Hoshino, H., Takaku, K., Nakajima, O., Muto, A., Suzuki, H., Tashiro, S., Takahashi, S., Shibahara, S., Alam, J., et al. (2002). Hemoprotein Bach1 regulates enhancer availability of heme oxygenase-1 gene. EMBO J. *21*, 5216–5224.

Sun, J., Brand, M., Zenke, Y., Tashiro, S., Groudine, M., and Igarashi, K. (2004). Heme regulates the dynamic exchange of Bach1 and NF-E2-related factors in the Maf transcription factor network. Proc. Natl. Acad. Sci. USA *101*, 1461–1466.

Tachibana, M., Sugimoto, K., Fukushima, T., and Shinkai, Y. (2001). Set domain-containing protein, G9a, is a novel lysine-preferring mammalian histone methyltransferase with hyperactivity and specific selectivity to lysines 9 and 27 of histone H3. J. Biol. Chem. *276*, 25309–25317.

Tahara, T., Sun, J., Igarashi, K., and Taketani, S. (2004a). Heme-dependent up-regulation of the alpha-globin gene expression by transcriptional repressor Bach1 in erythroid cells. Biochem. Biophys. Res. Commun. *324*, 77–85.

Tahara, T., Sun, J., Nakanishi, K., Yamamoto, M., Mori, H., Saito, T., Fujita, H., Igarashi, K., and Taketani, S. (2004b). Heme positively regulates the expression of beta-globin at the locus control region via the transcriptional factor Bach1 in erythroid cells. J. Biol. Chem. *279*, 5480–5487.

Takahashi, H., McCaffery, J.M., Irizarry, R.A., and Boeke, J.D. (2006). Nucleocytosolic acetyl-coenzyme a synthetase is required for histone acetylation and global transcription. Mol. Cell *23*, 207–217.

Wacker, D.A., Ruhl, D.D., Balagamwala, E.H., Hope, K.M., Zhang, T., and Kraus, W.L. (2007). The DNA binding and catalytic domains of poly(ADP-ribose) polymerase 1 cooperate in the regulation of chromatin structure and transcription. Mol. Cell. Biol. *27*, 7475–7485.

Wellen, K.E., Hatzivassiliou, G., Sachdeva, U.M., Bui, T.V., Cross, J.R., and Thompson, C.B. (2009). ATP-citrate lyase links cellular metabolism to histone acetylation. Science *324*, 1076–1080.

Xia, M., Chen, Y., Wang, L.C., Zandi, E., Yang, H., Bemanian, S., Martínez-Chantar, M.L., Mato, J.M., and Lu, S.C. (2010). Novel function and intracellular localization of methionine adenosyltransferase 2 beta splicing variants. J. Biol. Chem. *285*, 20015–20021.

Zhang, J., Ohta, T., Maruyama, A., Hosoya, T., Nishikawa, K., Maher, J.M., Shibahara, S., Itoh, K., and Yamamoto, M. (2006). BRG1 interacts with Nrf2 to selectively mediate HO-1 induction in response to oxidative stress. Mol. Cell. Biol. *26*, 7942–7952.

# Cyclosporine A-Based Immunotherapy in Adult Living Donor Liver Transplantation: Accurate and Improved Therapeutic Drug Monitoring by 4-hr Intravenous Infusion

*Taizo Hibi, Minoru Tanabe, Ken Hoshino, Yasushi Fuchimoto, Shigeyuki Kawachi, Osamu Itano, Hideaki Obara, Masahiro Shinoda, Naoki Shimojima, Kentaro Matsubara, Yasuhide Morikawa, and Yuko Kitagawa*

**Background.** A paucity of data exists for evaluating therapeutic drug monitoring in association with clinical outcomes of cyclosporine A (CYA) treatment in living donor liver transplantation (LDLT).

**Methods.** A retrospective cohort analysis was conducted on 50 consecutive adult patients who underwent LDLT between 2001 and 2009 to investigate the feasibility and efficacy of 4-hr continuous intravenous infusion of CYA-based immunotherapy (4-hr CYA-IV, n=27) and compare the pharmacokinetic profile and short-term prognoses with an oral microemulsion formulation of CYA (CYA-ME, n=23).

**Results.** All patients in the 4-hr CYA-IV group reached target CYA peak by day 3 compared with only 22% in the CYA-ME group ($P<0.001$). Adjustability to achieve the target range was easier in the 4-hr CYA-IV group compared with the CYA-ME group ($P=0.017$). Acute cellular rejection rate was lower in the 4-hr CYA-IV group (0%) compared with the CYA-ME group (17%, $P=0.038$). A subset analysis of the CYA-ME group revealed that CYA exposure was affected by external bile output ($P=0.006$). Patients in the CYA-ME group showed increased risk of switch to tacrolimus (35%) compared with the 4-hr CYA-IV group (7%, $P=0.030$). Toxicities and mortality rates were equivalent. The optimal initial dose of oral CYA at conversion from the 4-hr CYA-IV was considered to be 3-fold greater than that of the intravenous dose.

**Conclusions.** In LDLT, our 4-hr CYA-IV immunosuppression protocol was superior to CYA-ME oral dosing and allowed accurate therapeutic drug monitoring with excellent patient compliance.

**Keywords:** Cyclosporine A, Immunosuppression, Living donor liver transplantation, Therapeutic drug monitoring, Rejection.

(*Transplantation* 2011;92: 100–105)

Despite development of a wide range of novel drugs, calcineurin inhibitors (CNIs) remain the major agents for immunosuppression in liver transplantation. Tacrolimus (Tac) has been widely accepted for immunotherapy, whereas for patients unable to tolerate Tac, cyclosporine A (CYA) has been described as a valuable rescue therapy (*1–3*). One meta-analysis demonstrated that as a primary immunosuppressive agent, Tac was superior to CYA (including both the original oil-based formulation and the newer microemulsion formulation) in terms of mortality, graft loss, and rejection at 1 year (*4*). Nonetheless, all but one study included in this meta-analysis measured CYA trough levels to attain adequate levels of exposure (*4*).

Recently, Levy et al. (*5*) reported a randomized, multicenter study indicating decreased overall incidence of and statistically less severe acute cellular rejection in liver transplant recipients on an oral microemulsion formulation of CYA (CYA-ME) when 2-hr postdose levels were monitored, as a surrogate marker of CYA peak, instead of conventional CYA trough level. More importantly, a subset of patients in the 2-hr postdose monitoring group who reached the minimum target CYA peak range by day 3 demonstrated a significantly lower incidence of acute cellular rejection compared with patients who only achieved the target peak level by days

The authors declare no conflicts of interest.

Department of Surgery, Keio University School of Medicine, Shinjuku-ku, Tokyo, Japan.

Address correspondence to: Minoru Tanabe, M.D., Ph.D., Department of Surgery, Keio University School of Medicine, 35 Shinanomachi, Shinjuku-ku, Tokyo 160-8582, Japan.

E-mail: m-tanabe@sc.itc.keio.ac.jp

T.H., M.T., K.H., S.K., M.S., and Y.K. contributed to concept and design; T.H., M.T., K.H., S.K., O.I., M.S., and Y.M. participated in data analysis and interpretation; T.H. participated in drafting article; M.T., Y.M., and Y.K. participated in critical revision of article; T.H., S.K., and M.S. participated in statistics; T.H., S.K., H.O., M.S., N.S., and K.M. participated in data collection; and T.H., M.T., K.H., Y.F., S.K., O.I., H.O., M.S., N.S., K.M., Y.M., and Y.K. participated in approval of article.

Received 13 January 2011. Revision requested 1 February 2011.

Accepted 3 April 2011.



ISSN 0041-1337/11/9201-100

DOI: 10.1097/TP.0b013e31821dcae3

7 and 10, suggesting that reaching target levels at an early stage after transplant is crucial when a 2-hr postdose monitoring strategy is to be implemented (*5*). Subsequently, several randomized trials including the LIS2T study have reported promising results in terms of efficacy, toxicity, and pharmacoeconomics with CYA-ME, showing equivalent results in patient groups receiving CYA-ME with 2-hr postdose monitoring or Tac for patient and graft survivals and the overall incidence of acute rejection (*6–8*).

Nevertheless, data collected for the previous studies were generally based on deceased donor liver transplantations, and these results cannot be simply applied to adult living donor liver transplantation (LDLT). The reduced size of graft livers (usually hemi-liver), prolonged intestinal paralysis because of lengthy operation, and posttransplant external bile diversion described in recent publications from high-volume LDLT centers mostly in Japan (*9–12*) are the distinctive features of adult LDLT, contributing to delayed graft functional recovery and poor enteral absorption, which in turn substantially interfere with achieving and maintaining the therapeutic CYA peak blood concentration mentioned earlier.

To overcome these problems, intravenous CYA infusion may become a promising option because of its ability to ensure sufficient CYA exposure to exert immunosuppressive effects regardless of enteral absorption and biliary drainage. Clinical evidence of the efficacy and safety of intravenous CYA in liver transplantation is scarce, and appropriate therapeutic drug monitoring remains to be elucidated (*13, 14*). Moreover, no study has compared the clinical outcomes of intravenous infusion of CYA (CYA-IV) with CYA-ME regimens in LDLT to date. In the era of individually tailored immunosuppression, establishing a standard intravenous CYA protocol in LDLT is paramount, as an alternative CNI-based immunotherapy with potential advantages over Tac with regard to posttransplant new-onset diabetes mellitus and in the treatment of transplant patients with hepatitis C virus (HCV) or primary biliary cirrhosis and as a salvage immunosuppressive regimen in cases of Tac-related side effects (*15–17*). In this study, we evaluated the feasibility and efficacy of 4-hr intravenous CYA immunotherapy for LDLT, focusing on its therapeutic drug monitoring in comparison with a CYA-ME regimen.

## RESULTS

### Patient Demographics

The CYA-ME (Neoral, Novartis Pharma K. K., Tokyo, Japan, n=23) group and the 4-hr continuous intravenous infusion of CYA (4-hr CYA-IV; Sandimmun, Novartis Pharma K. K., n=27) groups were comparable for age, indications, Child-Pugh grade, model for end-stage liver disease scores, preoperative conditions, Eastern Cooperative Oncology Group performance status, graft lobe, graft:recipient weight ratio, graft volume/recipient standard liver volume, donor age, and blood loss (Table 1). The number of males in the CYA-ME group was higher compared with that in the 4-hr CYA-IV group ($P=0.035$; Table 1). Regarding surgical factors, the proportion of patients who underwent duct-to-duct reconstructions was higher ($P=0.044$), and cold and warm ischemia times were longer ($P=0.002$ and $P<0.001$, respectively) in the 4-hr CYA-IV group compared with those in the CYA-ME group (Table 1).

**TABLE 1.** Patient demographics

| Variables | CYA-ME | 4-hr CYA-IV | *P* |
|---|---|---|---|
| Total | 23 (100) | 27 (100) | |
| Age (yr) | 47±9 | 50±12 | 0.47 |
| Gender | | | |
| Male | 17 (74) | 12 (44) | 0.035 |
| Female | 6 (26) | 15 (56) | |
| Indication for LDLT | | | |
| HCV | 8 (35) | 9 (33) | 1.00 |
| HBV | 2 (9) | 3 (11) | |
| FHF | 2 (9) | 3 (11) | |
| PBC | 3 (13) | 3 (11) | |
| PSC | 1 (4) | 1 (4) | |
| Alcohol | 3 (13) | 3 (11) | |
| Others | 4 (17) | 5 (19) | |
| Child–Pugh grade | | | |
| A | 0 (0) | 1 (4) | 0.27 |
| B | 6 (26) | 3 (11) | |
| C | 17 (74) | 23 (85) | |
| MELD score | 19±6 | 17±6 | 0.49 |
| Preoperative condition | | | |
| Outpatient | 13 (57) | 15 (56) | 1.00 |
| Hospitalized | 7 (30) | 8 (30) | |
| ICU | 3 (13) | 4 (15) | |
| ECOG performance status | | | |
| 0–2 | 17 (74) | 17 (63) | 0.41 |
| 3, 4 | 6 (26) | 10 (37) | |
| Graft lobe | | | |
| Left (±caudate lobe) | 10 (43) | 17 (63) | 0.17 |
| Right | 13 (57) | 10 (37) | |
| GRWR | 0.90±0.27 | 0.90±0.21 | 0.92 |
| GV/RSLV (%) | 46±10 | 47±11 | 0.86 |
| Biliary reconstruction | | | |
| Duct-to-duct | 14 (61) | 24 (89) | 0.044 |
| Roux-en-Y | 9 (39) | 3 (11) | |
| Donor age (yr) | 41±15 | 38±12 | 0.35 |
| Cold ischemia time (min) | 53±22 | 80±32 | 0.002 |
| Warm ischemia time (min) | 45±10 | 63±14 | <0.001 |
| Blood loss (mL) | 4863±4424 | 5041±5873 | 0.91 |

Data are presented as N (%) and mean±standard deviation.

CYA-ME, oral microemulsion formulation of cyclosporine A; 4-hr CYA-IV, 4-hr continuous intravenous infusion of cyclosporine A; LDLT, living donor liver transplantation; HCV, hepatitis C virus; HBV, hepatitis B virus; FHF, fulminant hepatic failure; PBC, primary biliary cirrhosis; PSC, primary sclerotic cholangitis; MELD, model for end-stage liver disease; ICU, intensive care unit; ECOG, Eastern Cooperative Oncology Group; GRWR, graft:recipient weight ratio; GV/RSLV, graft volume/recipient standard liver volume.

### Pharmacokinetic Profiles of 4-hr CYA-IV and CYA-ME Groups

For the CYA-ME group, 9 of 15 patients (60%) who were not switched to other CNIs completed full pharmacokinetic evaluations on day 3. Of these nine patients, only two (22%) reached the target peak range of 700 to 1000 ng/mL (2-hr postdose CYA level 484±272 ng/mL; Fig. 1A). In con-